HU-EP-10/14

Light-like polygonal Wilson loops in 3d Chern-Simons and ABJM theory

Johannes M. Henn, Jan Plefka and Konstantin Wiegandt

Institut für Physik, Humboldt-Universität zu Berlin,
Newtonstraße 15, D-12489 Berlin, Germany
{henn,plefka,wiegandt}@physik.hu-berlin.de

Abstract

We study light-like polygonal Wilson loops in three-dimensional Chern-Simons and ABJM theory to two-loop order. For both theories we demonstrate that the one-loop contribution to these correlators cancels. For pure Chern-Simons, we find that specific UV divergences arise from diagrams involving two cusps, implying the loss of finiteness and topological invariance at two-loop order. Studying those UV divergences we derive anomalous conformal Ward identities for n-cusped Wilson loops which restrict the finite part of the latter to conformally invariant functions. We also compute the four-cusp Wilson loop in ABJM theory to two-loop order and find that the result is remarkably similar to that of the corresponding Wilson loop in $\mathcal{N} = 4$ SYM. Finally, we speculate about the existence of a Wilson loop/scattering amplitude relation in ABJM theory.

Contents

1 Introduction and conclusions **3**

2 One loop: Chern-Simons and ABJM theory **6**
2.1 Tetragon 7
2.2 Hexagon and higher polygons 8

3 Two loops: Chern-Simons theory **9**
3.1 Ladder diagrams 10
3.2 Vertex diagrams 10
3.3 Gauge field and ghost loops 12
3.4 Result for the two-loop tetragon in CS theory 12

4 Anomalous conformal Ward identities **12**
4.1 One-loop insertions 14
4.2 Two-loop insertions 15
4.2.1 Insertion into the ladder diagram 15
4.2.2 Insertion of the interaction term 16
4.2.3 Insertion of the kinetic term into the vertex diagram 16
4.2.4 Insertions with gauge field and ghost loops 17
4.3 Anomalous Ward identities and generalisation to higher polygons 18
4.4 Solution to the anomalous conformal Ward identities 19

5 Two loops: ABJM theory **19**
5.1 Gauge field contributions 19
5.2 Matter contributions 20

A Conventions **22**
A.1 Cherns-Simons theory and the Wilson loop operator 23
A.2 Lagrangian of ABJM theory 24

B Details of the two-loop calculation **25**
B.1 Vertex diagram 25
B.1.1 Numerical evaluation using the Mellin-Barnes method 26
B.2 Gauge field and ghost loops 29
B.2.1 Gauge field loop 29
B.2.2 Ghost loop 29
B.3 Conformal Ward identity 30
B.3.1 Insertion of the interaction term 30
B.3.2 Insertion of the kinetic term into the vertex diagram 31

C One loop gauge field propagator in ABJM theory **33**

1 Introduction and conclusions

Wilson loops are the central non-local observables in any gauge theory and thus of intrinsic interest. In 3d Chern-Simons theory they are the principal observables and topologically invariant with exactly known correlation functions [1] in the Euclidean (or Wick rotated) theory. This exact result is analytic in the inverse Chern-Simons parameter k and perturbative studies in a loop-expansion of the effective coupling constant $1/k$ can reproduce the exact topological and finite result to the first orders [2, 3], modulo regularisation subtleties leading to or not leading to an integer shift of k (for a review see [4]). Wilson loops in Minkowski-space with cusps and light-like segments, however, display particularly strong divergences in 4d gauge theories and seem to not have been considered in the 3d Chern-Simons literature before.

In this paper we study such light-like Wilson loops with cusps of polygonal shape in perturbation theory up to the next-to-leading order in $1/k$. We do this for both the pure 3d Chern-Simons theory as well as its conformal $\mathcal{N} = 6$ supersymmetric extension known as Aharony, Bergman, Jafferis, Maldacena (ABJM) theory [5]. The $\mathcal{N} = 6$ ABJM theory is built upon an $SU(N) \times SU(N)$ gauge symmetry which allows for a planar $N \to \infty$ limit with $\lambda = N/k$ held fixed, where k is the common absolute value of the Chern-Simons parameters of the two $SU(N)$ subgroups. In this limit the ABJM theory is conjectured to be dual to type IIA string theory on $AdS_4 \times \mathbb{CP}_3$, representing an exact gauge-string duality pair very similar in nature to the well studied 4d $\mathcal{N} = 4$ super Yang Mills/$AdS_5 \times S^5$ string duality pair. Supersymmetric Wilson loops in ABJM theory have been defined in [6–8] for the 1/6 BPS and recently in [9] for the 1/2 BPS case. The correlators for these loops of Euclidean, circular geometry are moreover known exactly in terms of a supermatrix model [10] using localisation techniques [11]. Our motivation to consider polygonal light-like Wilson loops in the 3d Chern-Simons ABJM gauge theory stems from the Wilson loop/scattering amplitude duality in $\mathcal{N} = 4$ super Yang-Mills. This duality was discovered in the dual $AdS_5 \times S^5$ string picture at strong gauge coupling in [12] and shown to exist also in the weak coupling regime [13–15] with profound consequences on the symmetries of these correlators leading to a dual superconformal [16] respectively Yangian symmetry [17] of scattering amplitudes, for reviews see [18, 19]. Moreover, there are many structural similarities of the 3d $\mathcal{N} = 6$ superconformal ABJM theory to $\mathcal{N} = 4$ super Yang-Mills, most notably the emergence of hidden integrability [20–23], (for reviews see [24–31]) in the planar limit for the spectral problem of determining anomalous scaling dimensions of local operators [32, 33].

Given these insights the question arises whether there could also be such a scattering amplitude/Wilson loop duality in the ABJM theory. Scattering amplitudes in the ABJM theory have been analysed by Agarwal, Beisert and McLoughlin [34] who in fact studied more general mass deformed superconformal Chern-Simons theories with extended supersymmetries at the one-loop order. There a vanishing result for the four-point one-loop amplitudes in the ABJM theory was found and the authors speculated whether the two-loop scattering amplitudes in $\mathcal{N} = 6$ Chern Simons (ABJM theory) could be simply related to the one-loop $\mathcal{N} = 4$ Yang-Mills amplitudes. The main result of our paper is that this picture is consistent at least up to the two-loop order:

We observe a cancellation of the one-loop graphs for null polygonal loops and find that the four-cusp Wilson loop at the two-loop order is of the same functional form as the four-point MHV amplitude of $\mathcal{N}=4$ up to constant numerical terms.

Specifically we calculate the expectation value of the n-cusped Wilson loop operator

$$\langle W_n \rangle := \frac{1}{N} \langle 0 | \operatorname{Tr} \mathcal{P} \exp \left(i \oint_{\mathcal{C}} A_\mu dz^\mu \right) | 0 \rangle \tag{1.1}$$

in the planar limit[1] for light-like polygonal contours $\mathcal{C}$ in pure Chern-Simons and ABJM theory, see Appendix A for conventions of the Lagrangian and the path ordering.

The contour of the n-sided polygon $\mathcal{C}$ is given by n points x_i $(i = 1, ..., n)$ where we parametrise each edge $\mathcal{C}_i$ via

$$z_i^\mu(s_i) = x_i^\mu + p_i^\mu s_i, \qquad\qquad p_i^\mu = x_{i+1}^\mu - x_i^\mu \tag{1.2}$$

where $s_i \in [\,0, 1\,]$ and $\mathcal{C} = \mathcal{C}_1 \cup ... \cup \mathcal{C}_n$. The calculations are performed in 3-dimensional Minkowski space with metric

$$\eta_{\mu\nu} = \operatorname{diag}(1, -1, -1)\,, \tag{1.3}$$

and the segments of the contour are light-like, i.e. $p_i^2 = 0$. Note that due to the light-like contour there is no difference in ABJM theory between the standard loop operator (1.1) above and the 1/6 BPS supersymmetric loop operator of [6], as the terms in the exponential coupling to the scalars drop out.

Wilson loops in Chern-Simons theory are usually defined with a framing procedure [1–3] which may be thought of as a widening of the Wilson line to a ribbon. This is necessary in order to define an integer twisting number of the individual loop and acts as a particular point-splitting regulator for collapsing gauge field propagators in perturbation theory while preserving the topological structure of the theory. Here we refrain from framing our loops as we do not encounter the problem of collapsing gauge field propagators due to the piece-wise linear structure of our loops. Moreover, the ABJM theory is not topological due to metric dependent interactions in the matter sector, so that there is no need for framing from that perspective either. Instead we regulate our correlators by the method of dimensional reduction which has been tested to the three-loop order in pure 3d Chern-Simons to yield a vanishing β-function and to satisfy the Slavnov-Taylor identities [35]. Here the tensor algebra is performed in 3 dimensions to obtain scalar integrands and then the dimension of the integrations are analytically continued.

The outcome of our computations at one-loop order in pure Chern-Simons and ABJM theory is that as claimed

$$\langle W_4 \rangle_{\text{1-loop}} = 0 \quad (\text{analytically})\,, \qquad \langle W_6 \rangle_{\text{1-loop}} = 0 \quad (\text{numerically})\,. \tag{1.4}$$

[1] I.e. we take the limit $N, k \to \infty$, $\frac{N}{k}$ finite.

Moreover, conformal Ward identities force $\langle W_n \rangle_{\text{1-loop}}$ to depend only on conformally invariant cross ratios of the $(x_i - x_j)^2$ and for $n = 4$ and 6 we show that these functions vanish.

At the two-loop order we computed the tetragonal Wilson-loop W_4 in pure Chern-Simons and $\mathcal{N} = 6$ superconformal Chern-Simons (ABJM theory). The result in dimensional reduction regularisation with $d = 3 - 2\epsilon$ for the correlator in pure planar Chern-Simons reads

$$\langle W_4 \rangle^{\text{CS}} = 1 - \left(\frac{N}{k}\right)^2 \left[\ln(2)\frac{(-x_{13}^2\,\tilde{\mu}^2)^{2\epsilon}}{2\epsilon} + \ln(2)\frac{(-x_{24}^2\,\tilde{\mu}^2)^{2\epsilon}}{2\epsilon} + \text{const.}\right] + \mathcal{O}[(\tfrac{N}{k})^3]\,. \tag{1.5}$$

We remark that this result displays a breakdown of finiteness and topological nature of the light-like four-cusp Wilson loop in 3d Chern-Simons at the two-loop order due to divergences[2] associated to two cusps at a light-like distance, see section 3.2. For the same correlator in the ABJM theory we find

$$\langle W_4 \rangle^{\text{ABJM}} = 1 + \left(\frac{N}{k}\right)^2 \left[-\left(\frac{(-\mu'^2\,x_{13}^2)^{2\epsilon}}{(2\epsilon)^2} + \frac{(-\mu'^2\,x_{24}^2)^{2\epsilon}}{(2\epsilon)^2}\right) + \frac{1}{2}\ln^2\left(\frac{x_{13}^2}{x_{24}^2}\right) + \text{const.}\right] + \mathcal{O}[(\tfrac{N}{k})^3]\,. \tag{1.6}$$

This is indeed of the same functional form as the one-loop result in $\mathcal{N} = 4$ super Yang-Mills theory, where one has [13]

$$\langle W_4 \rangle^{\mathcal{N}=4\ \text{SYM}} = 1 + \frac{g^2 N}{8\pi^2}\left[-\left(\frac{(-\mu^2\,x_{13}^2)^{\epsilon}}{\epsilon^2} + \frac{(-\mu^2\,x_{24}^2)^{\epsilon}}{\epsilon^2}\right) + \frac{1}{2}\ln^2\left(\frac{x_{13}^2}{x_{24}^2}\right) + \text{const.}\right] + \mathcal{O}[g^4 N^2]\,. \tag{1.7}$$

It would certainly be interesting to explore this relationship also beyond four cusps. Also a two-loop computation of the four-particle scattering amplitudes in ABJM theory would be very desirable in order to compare to our result.

From the string perspective the scattering amplitude/Wilson loop duality in the AdS_5/CFT_4 system arises from a combination of bosonic and fermionic T-dualities under which the free $AdS_5 \times S^5$ superstring is self-dual [36, 37]. Hence, for the existence of an analogue duality in ABJM theory one would require a similar self-duality of the $AdS_4 \times \mathbb{CP}_3$ superstring under a suitable combination of T-dualities. This problem was analysed by Adam, Dekal and Oz in [38] with a negative outcome: The Green-Schwarz σ-model is *not* self-dual under bosonic T-dualtities in the transverse AdS_4 directions combined with fermionic ones within the framework of the fermionic Buscher dualisation procedure employed in [36]. However, the analysis of [38] started from a partially κ-symmetry gauge fixed formulation of the $AdS_4 \times \mathbb{CP}_3$ superstring in terms of a supercoset σ-model [39, 40]. This restriction was overcome in [41] where, building upon a complete superspace formulation of $AdS_4 \times \mathbb{CP}_3$ [42], again the non-existence of a T-self-duality

[2]Regularisation is known to be a highly subtle issue in 3d Chern-Simons theory. In particular one could compute this correlator using a framing procedure adapted to light-like curves, which would be very interesting. We thank N. Drukker for discussions on this point.

of the $AdS_4 \times \mathbb{CP}_3$ superstring was found. Interestingly however, a very recent paper [43] has uncovered a Yangian symmetry of tree-level amplitudes in ABJM theory pointing towards integrability of the latter. Moreover, the authors argue about the possibility of a self-duality of the $AdS_4 \times \mathbb{CP}_3$ superstring upon T-dualizing also along the $\mathbb{CP}_3$ directions, which could provide a loop-hole for a scattering-amplitude/light-like Wilson loop duality of the ABJM theory. In order to settle this question a two-loop scattering amplitude computation in ABJM theory would be very desirable in order to compare to our result (1.6).

Our paper is organised as follows: In section 2 we perform the one-loop computation in pure Chern-Simons and ABJM theory for the tetragon and the hexagon Wilson loop. Section 3 is devoted to the two-loop problem of the tetragon in pure Chern-Simons theory where we compute all relevant graphs. Then, in section 4, we perform an independent check of our results by deriving anomalous conformal Ward identities for the Wilson loop. The latter can be generalised to an arbitrary number of points. In section 5 we include the matter diagrams arising in ABJM theory at the two-loop order and combine the results for the tetragon to obtain our final result (1.6). In the appendix we collect a detailed account of our conventions and give the technical details of the computation of the two-loop graphs using Mellin-Barnes techniques.

Note added

After publication of this paper the works [44], [45] appeared which report on a two loop calculation of four-point scattering amplitudes in ABJM theory. Most interestingly, the results coincide precisely with the divergent and finite pieces of our Wilson loop computation in (1.6) up to a constant. In the published version of this article there was an erroneous sign in (5.11) leading to a spurious sign difference between the Wilson loop and the scattering amplitude. We thank the authors of [45] for pointing this out to us.

2 One loop: Chern-Simons and ABJM theory

In this section we consider the one-loop expectation value of polygonal Wilson loops with n cusps. We would like to consider kinematical configurations for which all non-zero distances satisfy $-x_{ij}^2 > 0$, such that the result for the Wilson loops will be real (In particular, this allows us to drop the $i\epsilon$ prescription of the propagators). For n odd, however, it is impossible to find vectors p_i^μ that lead to such configurations. For this reason, we will only discuss n even.

At one-loop level, we only need terms quadratic in the expansion of the Wilson loop operator, and the free part of the action. Therefore, at one loop order, the expectation value of (1.1) in ABJM theory coincides with the one in pure Chern-Simons theory.

The expectation value at one loop is a sum over all possible diagrams where the propagator

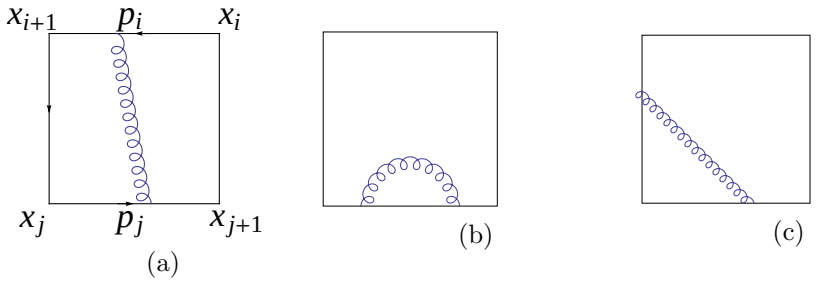

Figure 1: One-loop diagrams.

stretches between edges i and j,

$$\langle W(\mathcal{C})\rangle^{(1)} = \frac{(i)^2}{N}\sum_{i\geq j}\int ds_i ds_j \dot{z}_i^\mu \dot{z}_j^\nu \langle (A_\mu)_{mn}(z_i)\,(A_\nu)_{nm}(z_j)\rangle =: -\frac{N}{k}\frac{\Gamma\left(\frac{d}{2}\right)}{\pi^{\frac{d-2}{2}}}\sum_{i\geq j} I_{ij}\,, \tag{2.1}$$

where the domain of integration is given by $\int_0^1 ds_i \int_0^1 ds_j$ for $i \neq j$, $\int_0^1 ds_i \int_0^{s_i} ds_j$ for $i = j$ and $\dot{z}(s_i) = dz(s_i)/ds_i = p_i$ and where we have introduced a normalisation factor for later convenience. Here and throughout the paper, we absorb the dimensional regularisation scale $(\mu^2)^\epsilon$ into k and only display it explicitly in our final results. Using the Chern-Simons propagator in the Landau gauge[3]

$$\langle (A_\mu)_{mn}(x)\,(A_\nu)_{kl}(y)\rangle = \delta_{ml}\delta_{nk}\frac{1}{k}\left(\frac{\Gamma\left(\frac{d}{2}\right)}{\pi^{\frac{d-2}{2}}}\right)\epsilon_{\mu\nu\rho}\frac{(x-y)^\rho}{(-(x-y)^2)^{\frac{d}{2}}}\,, \tag{2.2}$$

and plugging in the expressions (1.2) for z_i, we obtain

$$I_{ij} = \int ds_i ds_j \frac{\epsilon(p_i, p_j, p_i s_i - p_j s_j + \sum_{k=j}^{i-1} p_k)}{\left(-x_{ij}^2 \bar{s}_i \bar{s}_j - x_{i+1,j}^2 s_i \bar{s}_j - x_{i,j+1}^2 \bar{s}_i s_j - x_{i+1,j+1}^2 s_i s_j\right)^{\frac{d}{2}}}\,, \tag{2.3}$$

where $x_{i,j}^2 = (x_i - x_j)^2$, $\bar{s}_i = 1 - s_i$ and $\epsilon(a,b,c) = \epsilon_{ijk}a^i b^j c^k$. We can immediately see that in this gauge $I_{i,i}$ and $I_{i,i+1}$ vanish due to the antisymmetry of the ϵ tensor. This corresponds to diagrams where the propagator ends on the same edge or on adjacent edges, as shown in Figures 1(b) and 1(c), respectively. Therefore we only need to keep diagrams of the type shown in Figure 1(a). The latter are manifestly finite in three dimensions and therefore we set $d = 3$ in the remainder of this section.

2.1 Tetragon

As explained above, in the Landau gauge, the only non-vanishing contributions to (2.1) for the tetragon are I_{31} and I_{42}. Setting $d = 3$, they are given by

$$I_{31} = -\epsilon(p_1, p_2, p_3)\int ds_1 ds_3 \frac{1}{(-x_{13}^2 \bar{s}_1 \bar{s}_3 - x_{24}^2 s_1 s_3)^{3/2}}\,, \tag{2.4}$$

[3]We drop the $i\epsilon$ prescription in the propagator, since we consider kinematical configurations with $-x_{ij}^2 > 0$.

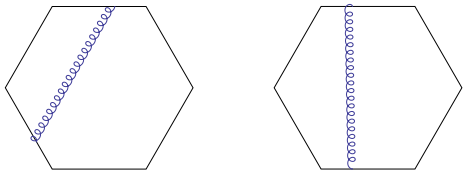

Figure 2: One-loop contributions $I_{i+2,i}$ and $I_{i+3,i}$ to the hexagonal Wilson loop.

and

$$I_{42} = -\epsilon(p_2, p_3, p_4) \int ds_2 ds_4 \frac{1}{(-x_{24}^2 \bar{s}_2 \bar{s}_4 - x_{13}^2 s_2 s_4)^{3/2}} \,. \tag{2.5}$$

Taking into account that we have a closed contour, i.e. $\sum_i p_i = 0$, we can write $\epsilon(p_2, p_3, p_4) = -\epsilon(p_2, p_3, p_1) = -\epsilon(p_1, p_2, p_3)$ and thus the contributions from the two diagrams cancel each other

$\langle W_4 \rangle^{(1)} \propto$ 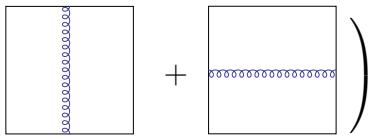 $= I_{31} + I_{42} = 0 \,.$ (2.6)

We will see in section 4 that this result is compatible with the restrictions imposed by conformal symmetry.

2.2 Hexagon and higher polygons

For the hexagon there are two different non-vanishing types of contributions, $I_{i+2,i}$ and $I_{i+3,i}$, as shown in Figure 2. The former appears in six orientations, $i = 1 \ldots 6$ (with the convention that $i + 6 \equiv i$), while the latter appears in three orientations, $i = 1, 2, 3$.

Specialising the general formula (2.3) to these cases we have

$$I_{i+2,i} = \int_0^1 ds_{i+2} ds_i \frac{\epsilon(p_{i+2}, p_i, p_{i+1})}{(-\bar{s}_i \bar{s}_{i+2} x_{i,i+2}^2 - s_i \bar{s}_{i+2} x_{i,i+3}^2 - s_i s_{i+2} x_{i+1,i+3}^2)^{3/2}} \tag{2.7}$$

and

$$I_{i+3,i} = \int_0^1 ds_{i+3} ds_i \frac{\epsilon(p_{i+3}, p_i, p_{i+1} + p_{i+2})}{(-\bar{s}_i \bar{s}_{i+3} x_{i,i+3}^2 - s_i \bar{s}_{i+3} x_{i+1,i+3}^2 - \bar{s}_i s_{i+3} x_{i,i+4}^2 - s_i s_{i+3} x_{i+1,i+4}^2)^{3/2}} \,. \tag{2.8}$$

We checked numerically for various non-symmetric hexagon configurations that the sum over all diagrams vanishes,

$$\langle W_6 \rangle^{(1)} \propto \sum_{i>j}^{6} I_{ij} = 0 \,. \tag{2.9}$$

Although we do not yet have an analytical proof for generic kinematical configurations, we can show that (2.9) is true for special configurations, as we will see presently.

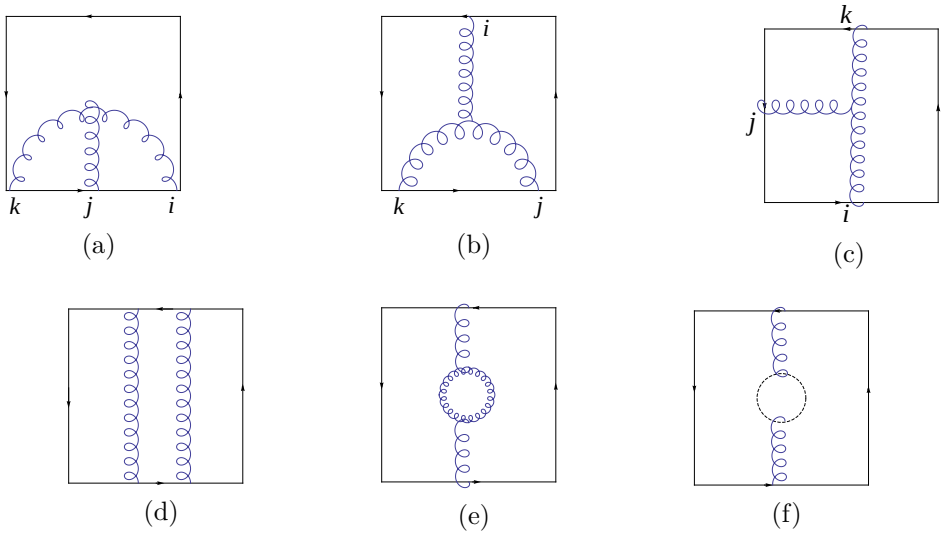

Figure 3: Planar two-loop topologies appearing in the polygonal Wilson loop in CS theory. Diagrams where one propagator is connected to a single edge or to two adjacent edges vanish in our gauge and are not displayed.

Consider the configuration where opposite edges are anti-parallel, i.e. $p_i = -p_{i+3}$. From (2.8) we see that $I_{i,i+3} = 0$ due to the antisymmetry of the ϵ tensor. Furthermore, taking into account that for this configuration we have $x^2_{i,i+2} = x^2_{i+3,i+5}$, it is easy to see from equation (2.7) that the integrands of $I_{i,i+2}$ and $I_{i+3,i+5}$ are the same. Finally, using $\sum_i p_i = 0$ one can see that the Levi-Civita symbols produce a differing sign, such that

$$I_{i,i+2} + I_{i+3,i+5} = \Big(\quad + \quad \Big)_{p_i = -p_{i+3}} = 0\,, \tag{2.10}$$

i.e. the contributions coming from those diagrams cancel pairwise, and we arrive at equation (2.9), in the specific anti-parallel kinematical configuration $p_i = -p_{i+3}$.

It is tempting to speculate that all n-cusped Wilson loops vanish at one-loop order in Chern-Simons theory.

3 Two loops: Chern-Simons theory

In the this section we calculate the two-loop contributions to the tetragonal light-like Wilson loop in pure Chern Simons theory. The results are consistent with the anomalous conformal Ward identity to be discussed in section 4.

Expanding the Wilson loop to quartic order, see (A.12), and performing Wick contractions leads to the topologies shown in Figure 3. We are taking the planar limit and therefore drop all non-planar graphs. Moreover, all diagrams where one propagator is connected to a single edge

or adjacent edges vanish in our gauge for the same reason as at the one-loop order and are not displayed.

3.1 Ladder diagrams

Let us begin by computing diagrams of ladder topology as shown in Figure 3d. There are two different orientations of this diagram, and it is easy to see that they give the same contribution. Taking into account this factor of 2, we have that the contribution of the ladder diagrams is

$$\langle W_4\rangle^{(2)}_{\text{ladder}} = 2\left(\frac{N}{k}\right)^2\left(\frac{\Gamma\left(\frac{d}{2}\right)}{\pi^{\frac{d-2}{2}}}\right)^2 I_{\text{ladder}}(x_{13}^2, x_{24}^2)\,, \tag{3.1}$$

where

$$I_{\text{ladder}}(x_{13}^2, x_{24}^2) = \int ds_{i,j,k,l}\frac{\epsilon(\dot z_i, \dot z_l, z_i - z_l)}{[-(z_i-z_l)^2]^{\frac{d}{2}}}\frac{\epsilon(\dot z_j, \dot z_k, z_j - z_k)}{[-(z_j-z_k)^2]^{\frac{d}{2}}}\,. \tag{3.2}$$

The integral is finite and may be calculated for $d = 3$

$$I_{\text{ladder}}(x_{13}^2, x_{24}^2) = \frac{1}{4}\int_0^1 ds_i\int_0^{s_i} ds_j\int_0^1 ds_k\int_0^{s_k} ds_l\frac{x_{13}^2x_{24}^2(x_{13}^2+x_{24}^2)}{[x_{13}^2\bar s_i\bar s_l + x_{24}^2 s_i s_l]^{\frac{3}{2}}[x_{13}^2\bar s_j\bar s_k + x_{24}^2 s_j s_k]^{\frac{3}{2}}} + O(\epsilon)\,. \tag{3.3}$$

We computed this integral by first carrying out some of the parameter integrals and then deriving a differential equation for it, which could be solved. The result is remarkably simple,

$$I_{\text{ladder}}(x_{13}^2, x_{24}^2) = \frac{1}{2}\left[\ln^2\left(\frac{x_{13}^2}{x_{24}^2}\right) + \pi^2\right] + O(\epsilon)\,. \tag{3.4}$$

Including the prefactors and dropping $O(\epsilon)$ terms, the contribution to the Wilson loop is

$$\langle W_4\rangle^{(2)}_{\text{ladder}} = \left(\frac{N}{k}\right)^2\frac{1}{4}\left[\ln^2\left(\frac{x_{13}^2}{x_{24}^2}\right) + \pi^2\right]\,. \tag{3.5}$$

3.2 Vertex diagrams

The diagrams with one three-gluon vertex shown in Figures 3a , 3b and 3c are obtained by contracting the cubic term in the expansion of the Wilson loop in (A.12) with the interaction term of the Lagrangian,

$$\langle W_4\rangle^{(2)}_{\text{vertex}} = \left(\frac{N}{k}\right)^2\frac{i}{2\pi}\left(\frac{\Gamma\left(\frac{d}{2}\right)}{\pi^{\frac{d-2}{2}}}\right)^3\sum_{i>j>k} I_{ijk}\,, \tag{3.6}$$

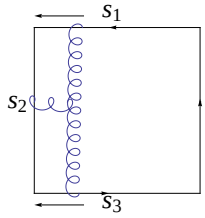

Figure 4: The divergence in the vertex diagram arises from the integration region where $s_1 \to 1, s_3 \to 0$ (and $\beta_1 \to 0, \beta_3 \to 0$), see equation (3.9).

where

$$I_{ijk} = -\int dz_i^\mu dz_j^\nu dz_k^\rho \epsilon^{\alpha\beta\gamma}\epsilon_{\mu\alpha\sigma}\epsilon_{\nu\beta\lambda}\epsilon_{\rho\gamma\tau}\int d^d w \frac{(w-z_i)^\sigma (w-z_j)^\lambda (w-z_k)^\tau}{|w-z_i|^d |w-z_j|^d |w-z_k|^d}\,, \tag{3.7}$$

and $|z_i| = (-z_i^2)^{\frac{1}{2}}$. Here the indices of I_{ijk} refer to the edges of the Wilson loop that the propagators attach to. The expression can be shown to be antisymmetric under the exchange of any two indices, and therefore the only non-vanishing contributions are the ones for $i \neq j \neq k$. As a consequence, topologies 3a and 3b can be discarded.

Specialising to the tetragon, we have four contributions which are symmetric under $x_{13}^2 \leftrightarrow x_{24}^2$ and thus it is sufficient to compute one of them

$$\begin{aligned} I_{321} &= \int d^d w \int_0^1 ds_{1,2,3} \frac{\epsilon(p_2,p_3,w)\epsilon(p_2,p_1,w)}{|w|^d |w-z_{12}|^d |w-z_{32}|^d} \\ &= \frac{i\pi^{\frac{d}{2}}}{8}\frac{\Gamma(d-1)}{\Gamma\left(\frac{d}{2}\right)^3} x_{13}^2 x_{24}^2 \int_0^1 d^3 s_{1,2,3} d^3\beta_{1,2,3} \left(\beta_1\beta_2\beta_3\right)^{\frac{d-2}{2}} \delta\left(\sum_{i=1}^3 \beta_i - 1\right) \times \\ &\qquad \times \left(\frac{1}{\Delta^{d-1}} - 2\frac{(d-1)}{\Delta^d}\beta_1\beta_3\bar{s}_1 s_3 (x_{13}^2 + x_{24}^2)\right)\,, \end{aligned} \tag{3.8}$$

where the second and third line is obtained by introducing Feynman parameters in the standard way and integrating over w. More details may be found in Appendix B.1. Δ is given by

$$\begin{aligned} \Delta &= -\beta_1\beta_2 z_{12}^2 - \beta_2\beta_3 z_{23}^2 - \beta_1\beta_3 z_{13}^2 \\ &= -x_{13}^2 \beta_1 \bar{s}_1 \left(\beta_3\bar{s}_3 + \beta_2 s_2\right) - x_{24}^2 \beta_3 s_3 \left(\beta_2 \bar{s}_2 + \beta_1 s_1\right) \end{aligned} \tag{3.9}$$

One might naively think that this diagram should give a finite answer due to the antisymmetry of the ϵ tensors. The result would indeed be finite in the case of smooth contours [2] or contours with a single cusp. However, the presence of two cusps gives rise to a region in the integration space of Feynman parameters where the first summand in the third line of (3.8) induces a divergent contribution. The relevant region of Feynman parameters is $s_1 \to 1, s_3 \to 0$ (and $\beta_1 \to 0, \beta_3 \to 0$), see equation (3.9), and is illustrated in Figure 4. Due to the presence of three independent vectors p_1^μ, p_2^μ and p_3^μ the ϵ tensors do not suppress this region. We find that this term produces a $1/\epsilon$ pole in dimensional reduction. The second summand in the third line of (3.8) is finite.

We separated the divergent and finite pieces using Mellin-Barnes techniques. The details can be found in Appendix B.1. We have not computed the coefficients of the ϵ^{-1} and ϵ^0 terms analytically, but we have good numerical evidence that they give the following result:

$$I_{321} = \frac{i\pi^{\frac{d}{2}+1}}{8}\frac{\Gamma(d-1)}{\Gamma\left(\frac{d}{2}\right)^3}\left[2\ln(2)\frac{(-x_{13}^2)^{2\epsilon}+(-x_{24}^2)^{2\epsilon}}{\epsilon}+\ln^2\left(\frac{x_{13}^2}{x_{24}^2}\right)+a_6+\mathcal{O}(\epsilon)\right] \tag{3.10}$$

where $a_6 = 8.354242685 \pm 2\cdot 10^{-9}$, see (B.27). Taking into account all prefactors and restoring the regularisation scale, $k \to \mu^{-2\epsilon}k$, we can write the result, up to terms of order ϵ, as

$$\langle W_4\rangle^{(2)}_{\text{vertex}} = -\left(\frac{N}{k}\right)^2\left[\frac{\ln(2)}{4}\sum_{i=1}^{4}\frac{(-x_{i,i+2}^2\,\mu^2\pi e^{\gamma_E})^{2\epsilon}}{\epsilon}+\frac{1}{4}\ln^2\left(\frac{x_{13}^2}{x_{24}^2}\right)+\frac{1}{4}a_6-2\ln(2)\right]. \tag{3.11}$$

3.3 Gauge field and ghost loops

It is well known [35] that in the dimensional reduction (DRED) scheme the gauge field loop diagrams shown in Figure 3e exactly cancel against the ghost loop diagrams shown in Figure 3f :

$$\langle W_4\rangle^{(2)}_{\text{gluon loop}} = -\langle W_4\rangle^{(2)}_{\text{ghost loop}}\,. \tag{3.12}$$

Details of this cancellation can be found in appendix B.2.

3.4 Result for the two-loop tetragon in CS theory

Summing up the results (3.5), (3.11) and (3.12) for the tetragon, interestingly, the $\ln^2(x_{13}^2/x_{24}^2)$ terms in the two-gauge-field diagram and the vertex diagram exactly cancel and we obtain

$$\langle W_4\rangle^{(2)} = -\left(\frac{N}{k}\right)^2\frac{1}{4}\left[\ln(2)\sum_{i=1}^{4}\frac{(-x_{i,i+2}^2\,\tilde{\mu}^2)^{2\epsilon}}{\epsilon}+a_6-8\ln(2)-\pi^2\right]. \tag{3.13}$$

where $\tilde{\mu}^2 = \mu^2\pi e^{\gamma_E}$ and we recall that $a_6 = 8.354242685 \pm 2\cdot 10^{-9}$. As we will see in the next section, the cancellation observed here that led to the finite part of (3.13) being a constant is in fact a consequence of the (broken) conformal symmetry of the Wilson loops under consideration.

4 Anomalous conformal Ward identities

The structure of the above results can be understood from conformal symmetry, by deriving anomalous conformal Ward identities for the Wilson loops. Here we follow very closely reference [46] .

We would like to use the specific properties of Wilson loops with light-like contours $\mathcal{C}$ under conformal transformations. The key point is that such contours are stable under conformal transformations, i.e. the deformed contour $\mathcal{C}'$ is also made of n light-like segments. This can be

seen as follows. The cusp points x_i form a contour with light-like edges, i.e. $x_{i,i+1}^2 = 0$. It is obvious that the light-likeness conditions are preserved by translations, rotations, and dilatations. Special conformal transformations are equivalent to an inversion $x_\mu \to x_\mu/x^2$ followed by a translation and another inversion. Thus it remains to investigate the transformation under inversions. Since under the latter $x_{ij}^2 \to x_{ij}^2/(x_i^2 x_j^2)$, it is clear that the light-likeness of the contour is preserved by all conformal transformations.

If the Wilson loop $\langle W_n \rangle$ were well defined in $d = 3$ dimensional Minkowski space it would enjoy the conformal invariance of the underlying gauge theory and we would conclude that $\langle W(\mathcal{C}) \rangle = \langle W(\mathcal{C}') \rangle$. This is indeed the case at one loop order, see section 2. However, as we have seen in section 3, starting from two loops, divergences force us to introduce a regularisation and calculate in $d = 3 - 2\epsilon$ dimensions, thereby breaking the conformal invariance of the action. The latter leads to an anomalous term in the conformal Ward identities for the Wilson loops, as we will see presently.

The expectation value of the Wilson loop can be written as a functional integral

$$\langle W_n \rangle = \int \mathcal{D}A \, e^{iS_\epsilon} \mathrm{Tr} \left[\mathcal{P} \exp \left(i \oint_{C_n} dz^\mu A_\mu(z) \right) \right] , \qquad S_\epsilon = \frac{1}{\mu^{2\epsilon}} \int d^d x \, \mathcal{L}_{\mathrm{CS}}(x) \tag{4.1}$$

where μ is the regularisation scale that keeps the action dimensionless in $d = 3 - 2\epsilon$. The path-ordered exponential is invariant under dilatations and the Lagrangian is covariant with weight $\Delta_{\mathcal{L}} = 3$, whereas the measure $d^d x$ does not match this weight for $d = 3 - 2\epsilon$. This results in a non-vanishing variation of the action with respect to dilatations and special conformal transformations. The conformal Ward identities can be derived by acting on both sides[4] of (4.1) with the generators of conformal transformations, see [46–48]. This leads to the Ward identities

$$\mathbb{D} \langle W_n \rangle = -\frac{2i\epsilon}{\mu^{2\epsilon}} \int d^d x \langle \mathcal{L}(x) W_n \rangle , \tag{4.2}$$

$$\mathbb{K}^\nu \langle W_n \rangle = -\frac{4i\epsilon}{\mu^{2\epsilon}} \int d^d x \, x^\nu \langle \mathcal{L}(x) W_n \rangle , \tag{4.3}$$

for dilatations and special conformal transformations. Here the operators on the left hand sides act in the canonical way on the coordinates of the cusp points,

$$\mathbb{D} = \sum_i (x_i \cdot \partial_i) , \qquad \mathbb{K}^\nu = \sum_i \left(2x_i^\nu (x_i \cdot \partial_i) - x_i^2 \partial_i^\nu \right) . \tag{4.4}$$

We emphasise that thanks to the factor of ϵ on the r.h.s. of (4.2) and (4.3) it is sufficient to know the divergent part of the integrals appearing on the r.h.s. of those equations in order to obtain information about the finite part of $\langle W_n \rangle$.

The dimensionally regularised Wilson loop $\langle W_n \rangle$ is a dimensionless scalar function of the cusp points x_i^ν, which appear paired with the regularisation scale as $x_{ij}^2 \mu^2$. As a consequence $\langle W_n \rangle$

[4]Note that the left-hand side of (4.1) is a function of the cusp points, whereas its right-hand side contains all fields of the Lagrangian.

satisfies

$$\left(\sum_{i=1}^{n}(x_i\cdot\partial_i)-\mu\,\frac{\partial}{\partial\mu}\right)\langle W_n\rangle=0\,. \tag{4.5}$$

This provides a consistency condition for the right hand side of (4.2).

4.1 One-loop insertions

At order N/k we have a contribution from the contraction of the kinetic part of the Lagrangian insertion with the second order expansion of the Wilson loop operator, shown in fig. 5,

$$\langle\mathcal{L}(x)W_n\rangle^{(1)}=\langle\mathcal{L}_{\rm kin}(x)W_n\rangle^{(1)}=\frac{(i)^2}{N}\int_{z_i>z_j}dz_{i,j}^{\mu,\nu}\epsilon^{\alpha\beta\gamma}\langle{\rm Tr}\,(A_\alpha\partial_\beta A_\gamma)(x){\rm Tr}\,(A_\mu A_\nu)\rangle^{(1)}\,. \tag{4.6}$$

The direct calculation of the right hand sides of (4.2) and (4.3), yields a vanishing result as

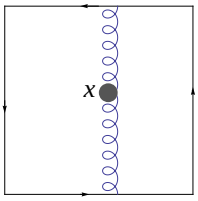

Figure 5: Lagrangian insertion contributing to the Ward identities at one loop.

$\epsilon\to 0$. Thus we have

$$\mathbb{D}\langle W_n\rangle^{(1)}=O(\epsilon)\,,\qquad\text{and}\qquad\mathbb{K}^\nu\langle W_n\rangle^{(1)}=O(\epsilon)\,, \tag{4.7}$$

in other words the conformal symmetry is unbroken for $\epsilon=0$. As a consequence, the expectation value of the Wilson loop is constrained to be a function of conformally invariant variables. Starting from the Lorentz invariants x_{ij}^2 the most general conformal invariants are the cross-ratios

$$u_{ijkl}:=\frac{x_{ij}^2x_{kl}^2}{x_{il}^2x_{jk}^2}\,. \tag{4.8}$$

In our case where neighbouring points are light-like separated, $x_{i,i+1}^2=0$, non-vanishing cross-ratios can only be written down starting from $n=6$. The special conformal Ward identities (4.7) then imply that $\langle W_n\rangle^{(1)}$ is given by a function of conformal cross-ratios,

$$\langle W_n\rangle^{(1)}=g_n\left(u_{ijkl}\right)\,,\qquad\langle W_4\rangle^{(1)}=const. \tag{4.9}$$

Since there are no non-vanishing conformal cross-ratios at four points, $\langle W_4\rangle^{(1)}$ must be a constant.

Let us now compare against the results of our one-loop computation of section 2. There, the constant on the r.h.s. of the second equation in (4.9) was found to be zero for the tetragon. Moreover, analytical investigations of certain symmetric contours and numerical investigations for non-symmetric contours show that $g_6(u_{ijkl})$ is zero for the hexagon. As mentioned before, we expect that the result remains true for higher polygons, i.e. $g_n=0$.

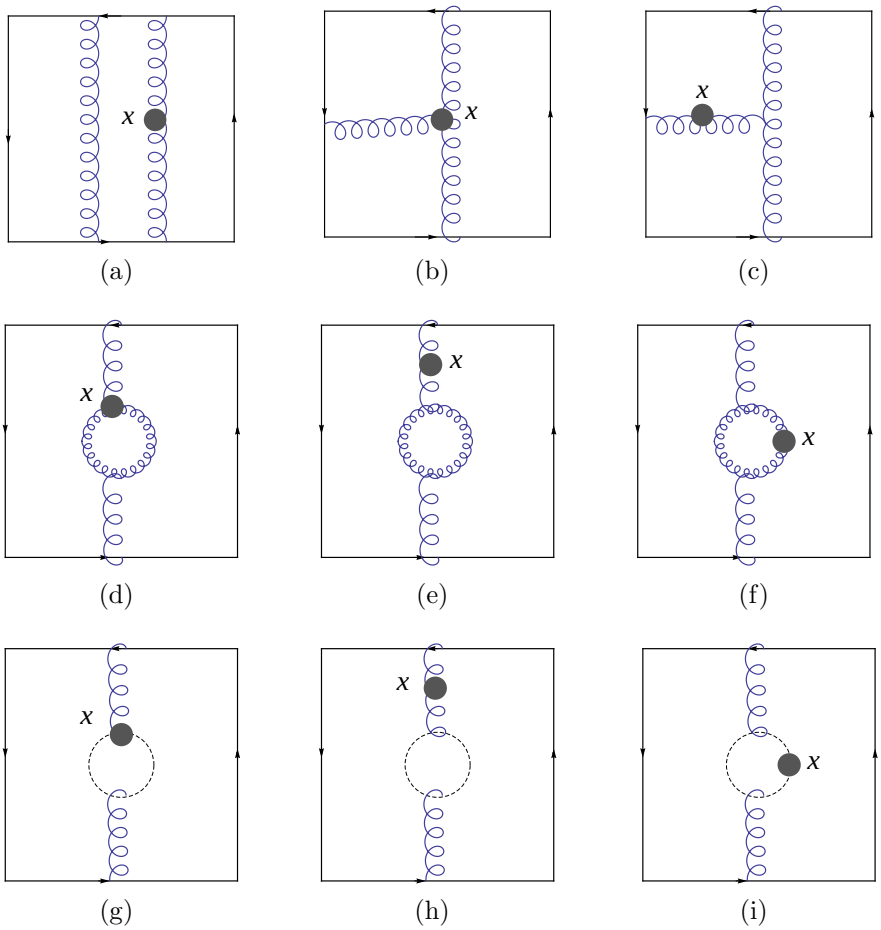

Figure 6: Two-loop contributions to the anomalous conformal Ward identity. The grey point in the pictures denotes the point x of the Lagrangian insertion in $\langle \mathcal{L}(x) W_n \rangle$. The diagrams of the second and third line cancel pairwise.

4.2 Two-loop insertions

At two loops there are several diagrams that contribute to the insertion of the Lagrangian into the Wilson loop, $\langle \mathcal{L}(x) W_n \rangle$, that correspond to the kinetic term, the gauge field vertex, the ghost kinetic term and the ghost vertex in $\mathcal{L}(x)$. Those diagrams are shown in Figure 6. We do not display diagrams that vanish for kinematical reasons as at one-loop level.

Just as at one-loop level, only diagrams giving rise to divergent integrals will contribute to the anomalous Ward identities.

4.2.1 Insertion into the ladder diagram

Let us consider the insertion of the kinetic term of the action into the ladder diagram as shown in Figure 6a. For the dilatation Ward identity these are exactly the two-gluon diagrams calculated

above, which are finite. For the special conformal Ward identity the integration is slightly more complicated, but the finiteness is easy to check for all contributions. Thus, this diagram does not contribute to the anomalous Ward identities.

4.2.2 Insertion of the interaction term

Next, we can contract the cubic order expansion of the Wilson loop with the vertex term of the Lagrangian insertion, as shown in Figure 6b,

$$\langle \mathcal{L}(x) W_4 \rangle^{(2)}_{(\mathrm{b})} = \langle \mathcal{L}_{\mathrm{int}}(x) \frac{1}{N} (i)^3 \int d^3 z^{\mu,\nu\rho}_{i,j,k} \,\mathrm{Tr}\, \left(A_\mu A_\nu A_\rho\right) \rangle \,. \tag{4.10}$$

For the dilatation Ward identity, we trivially have

$$\int d^d x \langle \mathcal{L}(x) W_4 \rangle^{(2)}_{(\mathrm{b})} = \frac{1}{i} \langle W_4 \rangle^{(2)}_{\mathrm{vertex}} = i \left(\frac{N}{k}\right)^2 \frac{\ln(2)}{\epsilon} + O(\epsilon^0) \,, \tag{4.11}$$

which is just the vertex diagram that was calculated in (3.6), up to a factor of i.

The contribution to the special conformal Ward identity is more complicated. We have

$$\int d^d x \, x^\nu \langle \mathcal{L}(x) W_4 \rangle^{(2)}_{(\mathrm{b})} = \left(\frac{N}{k}\right)^2 \frac{1}{2\pi} \left(\frac{\Gamma\left(\frac{d}{2}\right)}{\pi^{\frac{d-2}{2}}}\right)^3 \sum_{i>j>k} I'_{ijk} \tag{4.12}$$

with

$$I'_{321} = \int_0^1 ds_{1,2,3} \int d^d x (x + z_2)^\nu \frac{\epsilon(p_2, p_3, x)\epsilon(p_2, p_1, x)}{|x|^d |x - z_{12}|^d |x - z_{32}|^d} \tag{4.13}$$

$$= \frac{2\pi i \ln(2)}{\epsilon} (x_2 + x_3)^\nu + \mathcal{O}(\epsilon^0) \,, \tag{4.14}$$

where the coefficient $\ln(2)$ was computed numerically to 10 relevant digits. The reason the pole arises was discussed in section 3.2.

Details of this calculation can be found in appendix B.3.1. Summing up all four contributions $I'_{321}, I'_{421}, I'_{432}, I'_{431}$ we arrive at

$$\int d^d x \, x^\nu \langle \mathcal{L}(x) W_4 \rangle^{(2)}_{(\mathrm{b})} = \frac{i}{\epsilon} \left(\frac{N}{k}\right)^2 \frac{\ln(2)}{4} \sum_{i=1}^4 x_i^\nu \,. \tag{4.15}$$

4.2.3 Insertion of the kinetic term into the vertex diagram

Furthermore, we can contract one gauge field of the kinetic term of the insertion with the Wilson loop and the other one with the 3-gauge-field vertex, leading to a diagram of the type displayed

in Figure 6c,

$$\begin{aligned}\langle \mathcal{L}(x) W_4 \rangle^{(2)}_{(\mathrm{c})} &= \langle \mathcal{L}_{\mathrm{kin}}(x) \frac{1}{N} \oint_{z_i > z_j > z_k} dz^{\mu,\nu,\rho}_{i,j,k} \,\mathrm{Tr}\,\left(A_\mu A_\nu A_\rho\right) \left(i \int d^d w \mathcal{L}_{\mathrm{int}} \right) \rangle \\ &= \left(\frac{k}{4\pi}\right)^2 (i)^3 \frac{2}{3} \frac{1}{N} \int d^d x \int d^d w \oint dz^{\mu,\nu,\rho}_{i,j,k} \\ &\qquad \epsilon^{\alpha\beta\gamma} \epsilon^{\delta\sigma\tau} \langle \mathrm{Tr}\,\left(A_\alpha \partial_\beta A_\gamma\right)(x) \mathrm{Tr}\,\left(A_\mu A_\nu A_\rho\right) \mathrm{Tr}\,\left(A_\delta A_\sigma A_\tau\right)(w) \rangle \end{aligned} \tag{4.16}$$

Let us Wick-contract the kinetic term with $A_\nu(z_j)$ (the two other contractions are discussed below.) We obtain

$$\left(\frac{N}{k}\right)^2 \frac{i}{8\pi^2} \left(\frac{\Gamma\left(\frac{d}{2}\right)}{\pi^{\frac{d-2}{2}}} \right)^4 \int d^d w \oint dz^{\mu\nu\rho}_{i,j,k} \epsilon^{\delta\sigma\tau} I_{\nu\sigma} G_{\mu\tau}(z_i - w) G_{\rho\delta}(z_k - w) \,,$$

where $G_{\mu\nu} = \epsilon_{\mu\nu\rho}(x-y)^\rho / (-(x-y)^2)^{\frac{d}{2}}$ and where

$$I_{\nu\sigma}(x - z_j, x - w) = \epsilon^{\alpha\beta\gamma} \left[G_{\alpha\nu}(x - z_j) \partial^{(x)}_\beta G_{\gamma\sigma}(x - w) + G_{\alpha\sigma}(x - w) \partial^{(x)}_\beta G_{\gamma\nu}(x - z_j) \right] . \tag{4.17}$$

The only dependence on the insertion point x is in $I_{\nu\sigma}$. For the dilatation Ward identity the integral $\int d^d x \, I_{\nu\sigma}$ can easily be computed (for details see Appendix B.3.2) and effectively gives a propagator such that we have

$$\int d^d x \, \langle \mathcal{L}(x) W_4 \rangle^{(2)}_{(\mathrm{c})} = 3i \langle W_4 \rangle^{\mathrm{vertex}} = -3i \left(\frac{N}{k}\right)^2 \frac{\ln(2)}{\epsilon} + O(\epsilon^0) \,, \tag{4.18}$$

where a factor of 3 was included since the insertion can be in any of the 3 propagators of the vertex diagram and thus we get three times the same contribution.

The contribution to the special conformal Ward identity is more complicated, since the integration $\int d^d x \, x^\nu I_{\nu\sigma}$ does not just yield a propagator. Performing the calculation, we find

$$\int d^d x \, x^\nu \langle \mathcal{L}(x) W_4 \rangle^{(2)}_{(\mathrm{c})} = -\frac{i}{\epsilon} \left(\frac{N}{k}\right)^2 \frac{3}{4} \ln(2) \sum_{i=1}^{4} x^\nu_i + O(\epsilon^0) \,, \tag{4.19}$$

where the coefficient $\ln(2)$ was computed numerically (details can be found in Appendix B.3.2).

4.2.4 Insertions with gauge field and ghost loops

The gauge-field-ghost-insertions in Figure 6 cancel pairwise. For the dilatation Ward identity the insertions of the three gauge-field and the gauge-field-ghost vertices as shown in diagrams 6d, 6g are identical to the gauge field and ghost loop diagrams (3.12) and thus cancel. It is not necessary to perform the integration over the insertion point to see how the cancellation occurs and thus the contributions to the special conformal Ward identity cancel as well (for details on the cancellation see B.2).

Insertions of the kinetic term into the gauge field propagator as shown in diagrams 6e, 6h cancel as well, since the insertion is the same for both diagrams and thus the algebraic relations responsible for the cancellation in (3.12) remain unchanged.

Inserting gauge field respectively ghost kinetic terms into the propagators inside the loop in diagrams 6f, 6i produce slightly more complicated expressions. Nevertheless they cancel as well as can be seen in a straightforward calculation. For the dilatation Ward identity the cancellation can be seen in an even simpler way by noticing that the integration over the insertion point x effectively yields a gauge field respectively ghost propagator. Thus the diagrams are identical to the ones in (3.12) and cancel.

4.3 Anomalous Ward identities and generalisation to higher polygons

Summing up the divergent contributions of (4.11) (4.18), and inserting them into the dilatation Ward identity (4.2), we obtain

$$\mathbb{D}\langle W_4\rangle^{(2)} = -\left(\frac{N}{k}\right)^2 \ln(2)\left(\sum_{i=1}^{4} 1\right) + \mathcal{O}(\epsilon)\,, \tag{4.20}$$

where we have written the factor 4 as $(\sum_{i=1}^{4} 1)$ to emphasise its origin from the sum of four vertex-type diagrams. Note that only the divergent part of the vertex-diagram was required here. Summing up (4.15) and (4.19), and inserting them into the special conformal Ward identity (4.3), we obtain

$$\mathbb{K}^\nu\langle W_4\rangle^{(2)} = -2\left(\frac{N}{k}\right)^2 \ln(2)\sum_{i=1}^{4} x_i^\nu + \mathcal{O}(\epsilon)\,. \tag{4.21}$$

Let us now explain how these equations can be generalised from $n = 4$ to arbitrary n. In our two-loop computation, we found that the only diagrams contributing to (4.20) and (4.21) are those producing poles in ϵ. The mechanism for how these poles are generated was described in section 3.2, see in particular Figure 4. It is clear that for $n > 4$ cusps, the same type of vertex diagram will produce the divergent terms. Although those diagrams will depend on one further kinematical variable w.r.t. the four-point case, this dependence cannot change the (leading) UV pole ϵ^{-1} of the diagrams. Since there are n diagrams of this type at n points, we expect

$$\mathbb{D}\langle W_n\rangle^{(2)} = -\left(\frac{N}{k}\right)^2 \ln(2)\left(\sum_{i=1}^{n} 1\right) + \mathcal{O}(\epsilon)\,, \tag{4.22}$$

and

$$\mathbb{K}^\nu\langle W_n\rangle^{(2)} = -2\left(\frac{N}{k}\right)^2 \ln(2)\sum_{i=1}^{n} x_i^\nu + \mathcal{O}(\epsilon),\,. \tag{4.23}$$

We will now proceed to discuss the solution of these Ward identities and compare them to the result of the two-loop computation of the tetragon Wilson loop in section 3.4.

4.4 Solution to the anomalous conformal Ward identities

Using $\mathbb{D}\left(x_{ij}^2\right) = 2x_{ij}^2$ it is clear that the most general solution to the dilatation Ward identity (4.22) is

$$\langle W_n \rangle^{(2)} = -\left(\frac{N}{k}\right)^2 \left[\frac{\ln(2)}{4}\sum_{i=1}^{4}\frac{(-x_{i,i+2}^2\tilde{\mu}^2)^{2\epsilon}}{\epsilon} + f_n\left(\frac{x_{ij}^2}{x_{kl}^2}\right)\right] + O(\epsilon)\,, \tag{4.24}$$

where f is an arbitrary function of dimensionless variables and we recall that $\tilde{\mu}^2 = \mu^2\pi e^{\gamma_E}$. Of course, this is exactly what we expect from (4.5).

The result for the special conformal Ward identity is more interesting. Plugging (4.24) into the special conformal Ward identity (4.21) and using $\mathbb{K}^\nu \ln(x_{kl}^2) = 2(x_k + x_l)^\nu$, it is easy to see that the function f_n is allowed to depend on conformally invariant cross-ratios only, i.e. $f_n(x_{ij}^2/x_{kl}^2)$ $= g(u_{abcd})$. Therefore we finally have

$$\langle W_n \rangle^{(2)} = -\left(\frac{N}{k}\right)^2 \left[\frac{\ln(2)}{4}\sum_{i=1}^{n}\frac{(-x_{i,i+2}^2\tilde{\mu}^2)^{2\epsilon}}{\epsilon} + g_n(u_{abcd}) + \mathcal{O}(\epsilon)\right]. \tag{4.25}$$

In the four-point case, there are no non-vanishing cross-ratios, and therefore in particular g_4 must be a constant. This is in agreement with (3.13) and thus represents an independent check of the direct perturbative computation, including its finite part (recall that deriving the Ward identity does not rely on the finite parts of the direct perturbative computation). So, even though the result for the vertex diagram (3.11) was obtained numerically, its functional form is an analytical result, since we know the analytical expression for the ladder diagram and the sum of vertex and ladder diagram through the solution to the anomalous conformal Ward identity.

5 Two loops: ABJM theory

Here we explain how the results are modified in ABJM theory. We use the Wilson loop operator proposed in [6]

$$\langle W(A,\hat{A})\rangle = \frac{1}{2N}\left\langle \mathrm{Tr}\,\mathcal{P}\exp\left(i\oint_{\mathcal{C}} A_\mu dz^\mu\right) + \hat{\mathrm{Tr}}\,\mathcal{P}\exp\left(i\oint_{\mathcal{C}}\hat{A}_\mu dz^\mu\right)\right\rangle. \tag{5.1}$$

Note that the sign(s) in the exponent(s) in (5.1) are correlated to corresponding signs in the Lagrangian by the requirement of gauge invariance, see Appendix A.

5.1 Gauge field contributions

In ABJM theory there is a second copy of the gauge field $\hat{A}_\mu$ with opposite sign in the Lagrangian (A.20). Up to a sign, the gauge field contributions for both gauge groups are identical at one loop,

$$\langle W\rangle_A^{(1)} = -\langle W\rangle_{\hat{A}}^{(1)}\,, \tag{5.2}$$

due to the different sign of the propagator for the second gauge field, $\langle A_\mu A_\nu\rangle = -\langle \hat{A}_\mu \hat{A}_\nu\rangle$. Thus, at one loop the diagrams cancel. This does not differ from the result of pure Chern-Simons theory, since the expectation value at one loop vanishes, as we found in section 2 for $n = 4, 6$.

At two loops, however, the sign has no effect, since the two-gluon diagram contains an even number of propagators and in the vertex diagram we have to take into account the sign of the interaction term as well. Therefore, the two-loop diagrams are identical

$$\langle W\rangle_A^{(2)} = \langle W\rangle_{\hat{A}}^{(2)} \tag{5.3}$$

Thus, up to two loops, the expectation value for pure gauge field contributions is the same in ABJM theory and Chern-Simons theory

$$\langle W(A,\hat{A})\rangle_{\text{gauge fields}} = \langle W(A)\rangle_{\text{CS}}\,. \tag{5.4}$$

5.2 Matter contributions

In pure Chern-Simons theory the one-loop correction to the gauge field propagator is zero, since the contributions of gauge fields and ghosts exactly cancel against each other, see (3.12).

In ABJM theory we have to take into account fermionic and bosonic matter in the loop. This gauge field self energy has been calculated in [49, 50, 6] and the corrected propagator reads[5]

$$G^{(1)}_{\mu\nu}(x) = \left(\frac{2\pi}{k}\right)^2 \frac{N\delta_I^I}{8}\frac{\Gamma(1-\frac{d}{2})\Gamma(\frac{d}{2})^2}{\Gamma(d-1)\,\pi^d}\left(\frac{\Gamma(d-2)}{\Gamma(2-\frac{d}{2})}\frac{\eta_{\mu\nu}}{(-x^2)^{d-2}} - \partial_\mu\partial_\nu\left(\frac{\Gamma(d-3)}{\Gamma(3-\frac{d}{2})}\frac{1}{4}\frac{1}{(-x^2)^{d-3}}\right)\right), \tag{5.5}$$

for details see Appendix C. We can drop the derivative term in (5.5) (it would not contribute to the gauge-invariant Wilson loop) and instead use the propagator

$$G^{(1)}_{\mu\nu}(x) = -\frac{1}{N}\left(\frac{N}{k}\right)^2 \pi^{2-d}\Gamma\left(\frac{d}{2}-1\right)^2 \frac{\eta_{\mu\nu}}{(-x^2)^{d-2}}\,, \tag{5.6}$$

which up to two small differences is the tree level $\mathcal{N} = 4$ SYM gluon propagator. The first difference is a trivial prefactor, and the second is that since we are at two loops, the power of $1/x^2$ is $1-2\epsilon$ here, as opposed to $1-\epsilon$ in the one-loop computation in $\mathcal{N} = 4$ SYM. Thus it is clear that the results will be very similar to the expectation value of the Wilson loop in $\mathcal{N} = 4$ SYM. The corresponding calculation in $\mathcal{N} = 4$ SYM was carried out in [13] and we briefly summarise the results.

As in $\mathcal{N} = 4$ SYM we have three classes of diagrams shown in figure 7. Diagram 7a vanishes due to the light-likeness of the edges, whereas 7b yields a divergent, and 7c yields a finite

[5]Recall that we absorbed the regularisation scale into the coupling constant: $k \to \mu^{-2\epsilon}k$

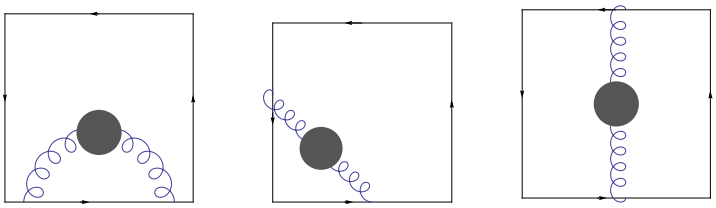

(a) (b) (c)

Figure 7: Examples for the three classes of diagrams involving the gauge field self energy: diagrams with (a) a propagator connecting the same edge (vanishing), (b) propagator stretching between adjacent edges (divergent), (c) propagator stretching between non-adjacent edges (finite). These diagrams have the same structure as the 1-loop diagrams in $\mathcal{N}=4$ SYM.

contribution. We have

$$\begin{aligned}\langle W_4\rangle^{(2)}_{\text{matter}} &= \frac{i^2}{N}\text{Tr}\int_{z_i>z_j} dz_i^\mu dz_j^\nu \langle A_\mu A_\nu\rangle^{(1)} \\ &= -N\sum_{i>j}\int ds_i ds_j p_i^\mu p_j^\nu G^{(1)}_{\mu\nu}(z_i-z_j) \\ &= \left(\frac{N}{k}\right)^2\left((4\pi e^{\gamma_E})^{2\epsilon}+\frac{\pi^2}{2}\epsilon^2+\mathcal{O}(\epsilon^3)\right)\sum_{i>j} I_{ij}\end{aligned} \tag{5.7}$$

where $I_{ij}=\int ds_i ds_j\, p_i\cdot p_j(-(z_i-z_j)^2)^{2-d}$.

There are four diagrams $I_{i+1,i}$ of the type shown in fig. 7b. It is sufficient to compute one of them, as the others can be obtained by the replacement $i\to i+1$. Setting e.g. $i=2,j=1$, we have

$$I_{21}=-\frac{1}{2}(-x_{13}^2)^{3-d}\int_0^1 ds_2 ds_1 \frac{1}{(\bar{s}_1 s_2)^{1-2\epsilon}}=-\frac{1}{8}\frac{(-x_{13}^2)^{2\epsilon}}{\epsilon^2} \tag{5.8}$$

Furthermore, there are two finite diagrams $I_{i+2,i}$ of the type shown in fig. 7c. Setting $d=3$ and taking $i=3,j=1$ we have

$$I_{31}=\frac{1}{2}\int_0^1 ds_3 ds_1 \frac{x_{13}^2+x_{24}^2}{x_{13}^2\bar{s}_1\bar{s}_3+x_{24}^2 s_1 s_3}=\frac{1}{4}\left[\ln^2\left(\frac{x_{13}^2}{x_{24}^2}\right)+\pi^2\right]. \tag{5.9}$$

Taking the sum over all contributions we obtain

$$\sum_{i>j} I_{ij}=\frac{1}{4}\left[-\frac{(-x_{13}^2)^{2\epsilon}}{\epsilon^2}-\frac{(-x_{24}^2)^{2\epsilon}}{\epsilon^2}+2\ln^2\left(\frac{x_{13}^2}{x_{24}^2}\right)+2\pi^2\right], \tag{5.10}$$

and thus the full matter part is

$$\langle W_4\rangle^{(2)}_{\text{matter}}=-\frac{1}{4}\left(\frac{N}{k}\right)^2\left[\frac{(-x_{13}^2 4\pi e^{\gamma_E}\mu^2)^{2\epsilon}}{\epsilon^2}+\frac{(-x_{24}^2 4\pi e^{\gamma_E}\mu^2)^{2\epsilon}}{\epsilon^2}-2\ln^2\left(\frac{x_{13}^2}{x_{24}^2}\right)-\pi^2+\mathcal{O}(\epsilon)\right], \tag{5.11}$$

where we have restored the regularisation scale μ^2. The full result is obtained by adding the CS part (3.13) to (5.11) and the result can be rewritten in a form in which the ϵ^{-1} terms cancel

$$\langle W_4\rangle^{(2)}_{\rm ABJM} = -\frac{1}{4}\left(\frac{N}{k}\right)^2\left[\frac{(-\mu'^2\,x_{13}^2)^{2\epsilon}}{\epsilon^2}+\frac{(-\mu'^2\,x_{24}^2)^{2\epsilon}}{\epsilon^2}-2\ln^2\left(\frac{x_{13}^2}{x_{24}^2}\right)-const.+\mathcal{O}(\epsilon)\right], \quad (5.12)$$

where $\mu'^2 = 8\pi e^{\gamma_E}\mu^2$ and $const. = 8\ln(2)+20\ln^2(2)+2\pi^2-a_6$ and where a_6 is given in (B.27) and fits the value $a_6 = -\frac{2}{3}\pi^2+16\ln(2)+8\ln^2(2)$ such that $const. = \frac{8}{3}\pi^2+12\ln^2(2)-8\ln(2)$.[6] This is the result quoted in the introduction (1.6).

Acknowledgements

We are grateful to N. Beisert, D. Berman, H. Dorn, N. Drukker, C. Grosse Wiesmann, T. McLoughlin, P. Nair, D. Sorokin and T. Schuster for valuable comments and discussions. J.H. is grateful to the Institute for Advanced Study, Princeton, for hospitality during the final stage of this work. This work was supported by the Volkswagen Foundation.

A Conventions

An n-sided polygon can be defined by n points x_i $(i = 1, ..., n)$, with the edge i being the line connecting x_i and x_{i+1}. Defining

$$p_i^\mu = x_{i+1}^\mu - x_i^\mu \quad (A.1)$$

and parametrising the position z_i^μ on edge i with the parameter $s_i \in [0,1]$ we have

$$z_i^\mu(s_i) = x_i^\mu + p_i^\mu s_i\,. \quad (A.2)$$

Furthermore, we use the notation

$$\epsilon(p,q,r) = \epsilon_{\mu\nu\rho}p^\mu q^\nu r^\rho \qquad \text{and} \qquad \bar{s}_i = 1-s_i. \quad (A.3)$$

One can easily check that with the definition $x_{ij}^\mu = x_i^\mu - x_j^\mu$

$$2\,x_{ij}\cdot x_{mn} = x_{in}^2+x_{jm}^2-x_{im}^2-x_{jn}^2 \quad (A.4)$$

We consider 3-dimensional Minkowski space with metric

$$\eta_{\mu\nu} = \text{diag}\,(1,-1,-1)\,. \quad (A.5)$$

Using (A.4) we can rewrite the scalar products

$$2p_i\cdot p_j = x_{i,j+1}^2+x_{i+1,j}^2-x_{i,j}^2-x_{i+1,j+1}^2\,. \quad (A.6)$$

Furthermore, using the definition (A.2), one can easily show that

$$(z_i-z_j)^2 = x_{ij}^2\bar{s}_i\bar{s}_j+x_{i+1,j}^2 s_i\bar{s}_j+x_{i,j+1}^2\bar{s}_i s_j+x_{i+1,j+1}^2 s_i s_j\,. \quad (A.7)$$

[6] Note that the log(2) term has a different transcendentality than the other terms. It stems from the vertex diagrams of the pure CS part (3.13) of the Wilson loop.

A.1 Cherns-Simons theory and the Wilson loop operator

The Chern-Simons action

$$S_{\rm CS} = \frac{k}{4\pi}\int d^dx\,\epsilon^{\mu\nu\rho}\,{\rm Tr}\,\left(A_\mu\partial_\nu A_\rho - \frac{2}{3}iA_\mu A_\nu A_\rho\right) \tag{A.8}$$

and the Wilson loop operator

$$W[\,\mathcal{C}\,] = \frac{1}{N}{\rm Tr}\,\mathcal{P}\exp\left(i\oint_{\mathcal{C}}A_\mu dz^\mu\right)\,. \tag{A.9}$$

are invariant[7] under $SU(N)$ gauge transformations

$$A_\mu \to A'_\mu = g(x)\,(A_\mu + i\partial_\mu)\,g^{-1}(x)\,, \qquad g(x)\in SU(N) \tag{A.10}$$

if the path ordering[8] is defined as

$$\begin{aligned}
&\mathcal{P}\left(A_\mu\left(z(s)\right)A_\nu\left(z(s')\right)\right) = A_\mu\left(z(s)\right)A_\nu\left(z(s')\right) \qquad \text{for} \quad s>s'\,, \\
&\mathcal{P}\left(A_\mu\left(z(s)\right)A_\nu\left(z(s')\right)\right) = A_\nu\left(z(s')\right)A_\mu\left(z(s)\right) \qquad \text{for} \quad s<s'
\end{aligned} \tag{A.11}$$

and $s\in(0,1)$ parametrises the path along the curve $\mathcal{C}$. The path ordered exponential in the Wilson loop operator then has the expansion

$$\begin{aligned}
\mathcal{P}\exp\left(i\oint_{\mathcal{C}}A_\mu dz^\mu\right) = 1_{\rm N\times N} &+ i\oint_{\mathcal{C}}dz_i^\mu A_\mu + (i)^2\oint_{\mathcal{C}}dz_i^\mu\int^{z_i}dz_j^\nu A_\mu A_\nu \\
&+ (i)^3\oint_{\mathcal{C}}dz_i^\mu\int^{z_i}dz_j^\nu\int^{z_j}dz_k^\rho A_\mu A_\nu A_\rho \\
&+ (i)^4\oint_{\mathcal{C}}dz_1^\mu\int^{z_i}dz_j^\nu\int^{z_j}dz_k^\rho\int^{z_k}dz_l^\sigma A_\mu A_\nu A_\rho A_\sigma + \ \ldots\,.
\end{aligned} \tag{A.12}$$

Quantising the theory with the standard Fadeev-Popov procedure yields the gauge fixing and ghost action

$$\mathcal{S}_{\rm g.f.} = \frac{k}{4\pi}\int d^dx\,{\rm Tr}\,\left(\frac{1}{\xi}\left(\partial^\mu A_\mu\right)^2 + \bar{c}\left(\partial^\mu D_\mu\right)c\right) \tag{A.13}$$

where $D_\mu c = \partial_\mu c + i[A_\mu, c\,]$. In Landau gauge ($\xi=0$) the gauge field propagator reads

$$\left\langle\left(A_\mu\right)_{ij}(x)\left(A_\nu\right)_{kl}(y)\right\rangle = \delta_{il}\delta_{jk}\frac{1}{k}\left(\frac{\Gamma\left(\frac{d}{2}\right)}{\pi^{\frac{d-2}{2}}}\right)\epsilon_{\mu\nu\rho}\frac{(x-y)^\rho}{\left(-(x-y)^2\right)^{\frac{d}{2}}} \tag{A.14}$$

[7] More precisely, the action is invariant under infinitesimal transformations $g(x)=1+i\alpha(x)$ and transforms like $S\to S'+(2\pi k)\delta S$, where $\delta S = -\frac{1}{24\pi^2}\int d^dx\,\epsilon^{\mu\nu\rho}{\rm Tr}\,\left((\partial_\mu g^{-1})g(\partial_\nu g^{-1})g(\partial_\rho g^{-1})g\right)$ under finite transformations. Since δS takes integer values, $\exp(iS)$ is invariant under large gauge transformations for $k\in\mathbb{N}$.

[8] There are different conventions on the path ordering. They are equivalent, it is however important to choose the sign in the Wilson loop such that it is gauge invariant. Reversing the sign in the exponent of the Wilson loop does not just reverse the integration contour, due to the path ordering.

where we have rescaled the coupling constant $k \to \mu^{-2\epsilon}k$ and restore the dependence on the regularisation scale μ only in the final results. The ghost propagator is

$$\langle c(x)\bar{c}(y)\rangle = \delta_{il}\delta_{jk}\frac{1}{k}\left(\frac{\Gamma\left(\frac{d}{2}-1\right)}{\pi^{\frac{d-2}{2}}}\right)\frac{1}{\left(-(x-y)^2\right)^{\frac{d}{2}-1}}\,. \tag{A.15}$$

Note that the gauge field propagator is related to the ghost propagator by

$$\langle (A_\mu)_{ij}(x)\,(A_\nu)_{kl}(y)\rangle = \frac{1}{2}\epsilon_{\mu\nu\rho}\partial^\rho\langle c(x)\bar{c}(y)\rangle\,, \tag{A.16}$$

which can be used to see the cancellation of gauge field and ghost loop contributions to the one-loop gauge field propagator in a simple way.

The different conventions found in the literature on Chern-Simons theory deserve a short comment. One can show, that

$$\mathcal{S} = \frac{k}{4\pi}\int d^dx\,\mathrm{Tr}\left(A_\mu\partial_\nu A_\rho - \frac{2}{3}sA_\mu A_\nu A_\rho\right)\epsilon^{\mu\nu\rho}\,, \tag{A.17}$$

$$W(\mathcal{C}) = \frac{1}{N}\mathrm{Tr}\,\mathcal{P}\exp\left(s\oint_{\mathcal{C}}A_\mu dz^\mu\right) \tag{A.18}$$

are invariant (In the sense mentioned above) under gauge transformations

$$A_\mu \to A'_\mu = g(x)\left(A_\mu - \frac{1}{s}\partial_\mu\right)g^{-1}(x) \tag{A.19}$$

where s is a real or imaginary parameter. I.e. the sign in the Wilson loop and the Lagrangian are correlated through gauge invariance. Taking a hermitian gauge field $(A_\mu)^\dagger = A_\mu$ we can choose $s = i$, which corresponds to the choice used throughout this document.

All other conventions found in the literature can be obtained by rescaling the gauge field $A_\mu \to -A_\mu$, $A_\mu \to iA_\mu$ etc. Note however, that this changes factors in the Lagrangian, the gauge transformation, the covariant derivative and the Wilson loop. A sign difference in the Wilson loop only may also be due to a different definition of the path ordering (A.11).

A.2 Lagrangian of ABJM theory

The action of ABJM theory is

$$\mathcal{S}_{\mathrm{ABJM}} = \mathcal{S}_{\mathrm{CS}} + \mathcal{S}_{\mathrm{g.f.}} + \hat{\mathcal{S}}_{\mathrm{CS}} + \hat{\mathcal{S}}_{\mathrm{g.f.}} + \mathcal{S}_{\mathrm{matter}} \tag{A.20}$$

where $\tilde{\mathcal{S}}$ is obtained from $\mathcal{S}$ by replacing A_μ with the gauge field in the anti-fundamental representation $\hat{A}_\mu$ and letting $k \to -k$. Explicitly, we have

$$S_{\rm CS} + \hat{S}_{\rm CS} = \frac{k}{4\pi} \int d^3x\, \varepsilon^{\mu\nu\rho} \Big[\mathrm{Tr}(A_\mu \partial_\nu A_\rho - \frac{2}{3} i\, A_\mu A_\nu A_\rho) - \mathrm{Tr}(\hat{A}_\mu \partial_\nu \hat{A}_\rho - \frac{2}{3} i\, \hat{A}_\mu \hat{A}_\nu \hat{A}_\rho) \Big] \quad \text{(A.21)}$$

$$S_{\rm gf} + \hat{S}_{\rm gf} = \frac{k}{4\pi} \int d^3x \Big[\frac{1}{\xi}\, \mathrm{Tr}(\partial_\mu A^\mu)^2 - \mathrm{Tr}(\partial_\mu \bar{c}\, D_\mu c) - \frac{1}{\xi}\, \mathrm{Tr}(\partial_\mu \hat{A}^\mu)^2 + \mathrm{Tr}(\partial_\mu \bar{\hat{c}}\, D_\mu \hat{c}) \Big] \quad \text{(A.22)}$$

$$S_{\rm matter} = \int d^3x \Big[\mathrm{Tr}(D_\mu C_I\, D^\mu \bar{C}^I) + i\, \mathrm{Tr}(\bar{\psi}^I \not{D}\, \psi_I) \Big] + S_{\rm int} \quad \text{(A.23)}$$

The field content consists of two $U(N)$ gauge fields $(A_\mu)_{ij}$ and $(\hat{A}_\mu)_{\hat{i}\hat{j}}$, the complex fields $(C_I)_{i\hat{i}}$ and $(\bar{C}^I)_{\hat{i}i}$ as well as the fermions $(\psi_I)_{\hat{i}i}$ and $(\bar{\psi}^I)_{i\hat{i}}$ in the $(\mathbf{N}, \bar{\mathbf{N}})$ and $(\bar{\mathbf{N}}, \mathbf{N})$ of $U(N)$ respectively, $I = 1, 2, 3, 4$ is the $SU(4)_R$ index. We employ the covariant gauge fixing function $\partial_\mu A^\mu$ for both gauge fields and have two sets of ghosts $(\bar{c}, c)$ and $(\bar{\hat{c}}, \hat{c})$. $S_{\rm int}$ are the sextic scalar potential and $\Psi^2 C^2$ Yukawa type potentials spelled out in [5]. The covariant derivative is given by $D_\mu c = \partial_\mu c + i[A_\mu, .]$. It's action on Ψ^I, C^I is given in [6] and not needed here.

B Details of the two-loop calculation

B.1 Vertex diagram

Using $\epsilon(p_1, p_2, z_{12}) = \epsilon(p_3, p_2, z_{32}) = 0$ the first line in (3.8) can be rewritten as

$$I_{321} = \int d^3 s_{1,2,3} \epsilon(p_1, p_2, \partial_{z_1}) \epsilon(p_3, p_2, \partial_{z_3}) \int d^d w \frac{(d-2)^{-2}}{|w|^d |w - z_{12}|^{d-2} |w - z_{32}|^{d-2}}\,. \quad \text{(B.1)}$$

We begin by introducing Feynman parameters,

$$\int d^d w \frac{1}{|w|^d |w - z_{12}|^{d-2} |w - z_{32}|^{d-2}} = \int [d\beta]_3 \int d^d w \frac{1}{(-(w - \beta_1 z_{12} - \beta_3 z_{32})^2 + \Delta)^{(3d-4)/2}}\,, \quad \text{(B.2)}$$

where

$$\int [d\beta]_3 = \int_0^1 d\beta_1 d\beta_2 d\beta_3 (\beta_1 \beta_2 \beta_3)^{(d-2)/2-1} \beta_2 \delta(\sum_i \beta_i - 1) \frac{\Gamma(\frac{3d}{2} - 2)}{\Gamma(\frac{d}{2}) \Gamma(\frac{d}{2} - 1)^2} \quad \text{(B.3)}$$

and

$$\Delta = 2\beta_1 \beta_3 (z_{12} \cdot z_{32}) - z_{12}^2 \beta_1 \bar{\beta}_1 - z_{32}^2 \beta_3 \bar{\beta}_3\,. \quad \text{(B.4)}$$

Shifting the integration contour $w \to l = w - \beta_1 z_{12} - \beta_3 z_{32}$ we have a standard integral

$$\int d^d l \frac{1}{[l^2 - \Delta]^n} = (-1)^n i \pi^{d/2} \frac{\Gamma(n - \frac{d}{2})}{\Gamma(n)} \left(\frac{1}{\Delta} \right)^{n - \frac{d}{2}}\,. \quad \text{(B.5)}$$

Thus we get

$$I_{321} = \frac{c_1}{(d-2)^2} \int [d\beta]_3 d^3 s_{1,2,3} \epsilon(p_1, p_2, \partial_{z_1}) \epsilon(p_3, p_2, \partial_{z_3}) \frac{1}{\Delta^{d-2}}\,, \quad \text{(B.6)}$$

where $c_1 = i\pi^{\frac{d}{2}}\Gamma(d-2)/\Gamma(3d/2-2)$. Evaluating the action of the derivatives and abbreviating $x_{13}^2 = s, x_{24}^2 = t$ we obtain

$$I_{321} = c_2 st \int_0^1 d^3 s_{1,2,3} d^3\beta_{1,2,3} (\beta_1\beta_2\beta_3)^{(d-2)/2} \delta(\sum_i \beta_i - 1) \left(\frac{1}{\Delta^{d-1}} - 2\frac{(d-1)}{\Delta^d} \beta_1\beta_3 \bar{s}_1 s_3 (s+t)) \right) \tag{B.7}$$

where $c_2 = i\pi^{d/2}\Gamma(d-1)/(8\Gamma^3(d/2))$ and both terms are separately symmetric under $s \leftrightarrow t$. Performing the change of variables

$$\beta_1 = xy\,, \qquad \beta_2 = \bar{x}y\,, \qquad \beta_3 = \bar{y}\,, \qquad \sum_i \beta_i = 1 \qquad x, y \in [0,1] \tag{B.8}$$

with Jacobian y we can rewrite (B.38) in a form where all integrations range from 0 to 1,

$$\begin{aligned} I_A &= c_2 st \int_0^1 d^3 s dx dy \frac{(x\bar{x}\bar{y})^{\frac{d-2}{2}}}{\Delta_y^{d-1}}\,, \\ I_B &= -2(d-1)c_2 st(s+t) \int_0^1 d^3 s dx dy \frac{(x\bar{y})^{\frac{d}{2}} \bar{x}^{\frac{d-2}{2}} \bar{s}_1 s_3}{\Delta_y^d}\,, \end{aligned} \tag{B.9}$$

where

$$\Delta_y = -\left(sx\bar{s}_1(\bar{s}_3\bar{y} + s_2\bar{x}y) + t\bar{y}s_3(xs_1 + \bar{s}_2\bar{x}) \right)\,, \tag{B.10}$$

and $I_{321} = I_A + I_B$. The integral I_A is divergent as $\bar{s}_1, s_3 \to 0$, see also fig. 4

B.1.1 Numerical evaluation using the Mellin-Barnes method

In this section, we switch from the Feynman parametrization in equation (B.9) to a Mellin-Barnes representation, as the latter is very convenient to perform a systematic expansion in ϵ. An introduction to the Mellin Barnes technique can be found in [51].

In the first step the sum in the denominator is transformed into an integral over a product of terms. Since the denominator in (B.38) consists of a sum of four terms, we will introduce 3 Mellin parameters z_1, z_2, z_3. By repeated use of the Mellin-Barnes representation

$$\frac{1}{(X+Y)^\lambda} = \frac{1}{\Gamma(\lambda)} \frac{1}{2\pi i} \int_{\beta-i\infty}^{\beta+i\infty} \frac{Y^z}{X^{\lambda+z}} \Gamma(z+\lambda)\Gamma(-z) dz\,, \tag{B.11}$$

where $-\mathrm{Re}(\lambda) < \beta < 0$, one obtains

$$\frac{(2\pi i)^3 \Gamma(\lambda)}{(a+b+c+d)^\lambda} = \int dz_{1,2,3} a^{z_1} b^{z_2} c^{z_3} d^{-\lambda-z_1-z_2-z_3} \Gamma(-z_1)\Gamma(-z_2)\Gamma(-z_3)\Gamma(\lambda+z_1+z_2+z_3) \tag{B.12}$$

where the real parts β_i of the integration contour have to be chosen such that the arguments in all Γ functions have positive real part. Applying (B.12) to the denominator of I_A (B.9), we can rewrite I_A as

$$I_A = \frac{c_2}{\Gamma(d-1)} \int d\tilde{z}_{1,2,3} \Gamma(-z_1)\Gamma(-z_2)\Gamma(-z_3)\Gamma(d-1+z_1+z_2+z_3)(-s)^{z_1+z_2+1}(-t)^{-d-z_1-z_2+2} \tag{B.13}$$

$$\int d^3s dx dy s_1^{z_3} \bar{s}_1^{z_1+z_2} s_2^{z_2} \bar{s}_2^{-z_1-z_2-z_3-d+1} s_3^{-z_1-z_2-d+1} \bar{s}_3^{z_1} x^{z_1+z_2+z_3+d/2-1} \bar{x}^{-z_1-z_3-d/2} y^{z_2} \bar{y}^{-z_2-d/2}$$

where $d\tilde{z} = (2\pi i)^{-1} dz$. The integrals over s_1, s_2, s_3, x, y can be carried out using

$$\int_0^1 s_i^{a-1}(1-s_i)^{b-1} dt = \Gamma(a)\Gamma(b)/\Gamma(a+b)\,, \tag{B.14}$$

and we arrive at

$$\begin{aligned} I_A = \frac{c_2}{\Gamma(d-1)} \int d\tilde{z}_{1,2,3} (-s)^{z_1+z_2+1}(-t)^{-d-z_1-z_2+2} \Gamma(-z_1)\Gamma(-z_2)\Gamma(-z_3) \qquad \text{(B.15)} \\ \times \Gamma(z_1+1)\Gamma(z_2+1)\Gamma(z_3+1)\Gamma(d-1+z_1+z_2+z_3)\Gamma\left(-d/2-z_2+1\right)\Gamma(z_1+z_2+1) \\ \times \Gamma(-d-z_1-z_2+2)\Gamma\left(-d/2-z_1-z_3+1\right)\Gamma(-d-z_1-z_2-z_3+2)\Gamma\left(d/2+z_1+z_2+z_3\right) \\ \times \left[\Gamma\left(2-d/2\right)\Gamma(-d-z_2+3)\Gamma(-d-z_1-z_3+3)\Gamma(z_1+z_2+z_3+2)\right]^{-1}\,. \end{aligned}$$

Recall that we investigate the kinematical region where $s, t < 0$.

One can see that this integral is divergent as $\epsilon \to 0$ by noticing that for $\epsilon = 0$ it is impossible to choose the integration contours such that all poles of $\Gamma(...+z_1)$ are to the left of the integration contour and all poles of $\Gamma(...-z_1)$ are to the right of the contour. [9] The reason is that the poles of $\Gamma(z_1+z_2+1)$ and $\Gamma(-d-z_1-z_2-z_3+2) = \Gamma(-z_1-z_2-1+2\epsilon)$ "glue together" at $z_1 = -z_2-1$ for $\epsilon = 0$. However, one can find allowed contours for $\epsilon \neq 0$.

By shifting the contour left to the pole at $z_1 = -z_2 - 1$ we pick up a residue. The factor of $\Gamma(-z_1-z_2-1+2\epsilon)$ evaluated at the residue, results in a divergent factor of $\Gamma(2\epsilon)$. The remaining integral over the shifted contour yields a finite contribution.

The steps of shifting contours and taking residues have been automatised in [52] and we used this package to systematically extract the pole terms. Applying this procedure to (B.15) and expanding in ϵ yields 3 integrals:

$$I_A^{(1)} = c_2 \int \frac{dz_1}{2\pi i} \left(\frac{1}{\epsilon} + 2\log(-s) - g_1(z_1)\right) f_1(z_1) + \mathcal{O}(\epsilon) \tag{B.16}$$

$$I_A^{(2)} = c_2 \int \frac{dz_1 dz_3}{(2\pi i)^2} \left(\frac{1}{\epsilon} + 2\log(-s) - g_2(z_1,z_3)\right) f_2(z_1,z_3) + \mathcal{O}(\epsilon) \tag{B.17}$$

$$I_A^{(3)} = c_2 \int \frac{dz_1 dz_2 dz_3}{(2\pi i)^3} \left(\frac{s}{t}\right)^{1+z_1+z_2} f_3(z_1,z_2,z_3) \tag{B.18}$$

[9] This is necessary in order for the previous steps to be well-defined.

We do not specify the values of the real parts β_i as well as the functions f_i, g_i here, which are lengthy expressions of products of Γ functions and can be obtained automatically by expanding (B.15) with the help of [52]. Adding up the divergent part of (B.16) and (B.17) we get

$$I_{\text{div}}^{\text{vertex}} = \frac{a_1}{\epsilon} c_2 \tag{B.19}$$

where by numerical integration one finds

$$a_1 = \int \frac{dz_1}{2\pi i} f_1(z_1) + \int \frac{dz_1 dz_3}{(2\pi i)^2} f_2(z_1, z_3) = 8.710344 \pm 10^{-6} \approx 4\pi \ln(2) = 8.710344361\ldots \tag{B.20}$$

accurately approximated by our analytic guess. Further numerical evaluation of the finite part of $I_A^{(1)}$, $I_A^{(2)}$, $I_A^{(3)}$ yields

$$I_{A,\text{finite}} = c_2 \left(a_1 \ln(-s) + a_1 \ln(-t) + a_2 \ln^2\left(\frac{s}{t}\right) + a_4 \right) . \tag{B.21}$$

where a_1 has the same value as above and

$$a_2 = -0.84 \pm 0.01 \qquad a_4 = -14.375216465 \pm 10^{-9} . \tag{B.22}$$

Numerical analysis for I_B suggests

$$I_B = c_2 \left(a_3 \ln^2\left(\frac{s}{t}\right) + a_5 \right) \tag{B.23}$$

where

$$a_3 = 3.97 \pm 0.01 , \qquad a_5 = 40.620843911 \pm 10^{-9} . \tag{B.24}$$

Adding up a_2, a_3 we obtain

$$a_2 + a_3 = 3.136 \pm 0.02 \approx \pi . \tag{B.25}$$

Thus suggesting

$$\begin{aligned} I_A + I_B &= c_2 \left(\frac{a_1}{\epsilon} + a_1 \left(\ln(-s) + \ln(-t)\right) + (a_2 + a_3) \ln\left(\frac{s}{t}\right) + (a_4 + a_5) + \mathcal{O}(\epsilon) \right) \\ &\approx c_2 \pi \left(\frac{4\ln(2)}{\epsilon} + 4\ln(2) \left(\ln(-s) + \ln(-t)\right) + \ln^2\left(\frac{s}{t}\right) + a_6 + \mathcal{O}(\epsilon) \right) \end{aligned} \tag{B.26}$$

where

$$a_6 = (a_4 + a_5)/\pi = 8.354242685 \pm 2 \cdot 10^{-9} . \tag{B.27}$$

The constant fits the value $a_6 \approx -\frac{2}{3}\pi^2 + 16\ln(2) + 8\ln^2(2) = 8.35424273...$. The result can be rewritten in the form

$$I_A + I_B \approx c_2 \pi \left(2\ln(2) \frac{\left((-s)^{2\epsilon} + (-t)^{2\epsilon}\right)}{\epsilon} + \ln^2\left(\frac{s}{t}\right) + a_6 + \mathcal{O}(\epsilon) \right) \tag{B.28}$$

B.2 Gauge field and ghost loops

It is well known [35], that the contributions of ghost and gauge field loops to the gauge field self energy cancel. We briefly review the cancellation of the gauge field and ghost loop corrections in the Wilson loop, since from this it is easy to see, how the cancellation for the insertions in the conformal Ward identities takes place.

B.2.1 Gauge field loop

The gauge field loop-diagram arises at second order in perturbation theory

$$\begin{aligned}\langle W_n\rangle^{\text{gluon-loop}} &= \frac{1}{N}\langle \mathrm{Tr}\,(-\oint dz_i^\mu dz_j^\nu A_\mu A_\nu)\left(-\frac{1}{2!}\right)\left(\frac{k}{4\pi}\int d^dx \epsilon^{\alpha\beta\gamma}\mathrm{Tr}\,(\frac{2}{3}iA_\alpha A_\beta A_\gamma)\right)^2\rangle \qquad \text{(B.29)}\\ &= c_8\left(\frac{2}{3}\right)^2\oint dz_i^\mu dz_j^\nu\int d^dx d^dy \epsilon^{\alpha\beta\gamma}\epsilon^{\delta\sigma\tau}\langle \mathrm{Tr}\,(A_\mu A_\nu)\mathrm{Tr}\,(A_\alpha A_\beta A_\gamma)(x)\mathrm{Tr}\,(A_\delta A_\sigma A_\tau)(y)\rangle\end{aligned}$$

where

$$c_8 = -\frac{1}{N}\frac{1}{2}\left(\frac{k}{4\pi}\right)^2 . \qquad \text{(B.30)}$$

Taking into account that A_μ, A_ν give 3 identical contractions with one of the vertex terms and that we can contract them either with the x- or y-dependent vertex, we get a symmetry factor of $3\cdot 3\cdot 2$. The remaining contractions of the gauge fields are dictated by taking into account only planar diagrams. Thus we get

$$\langle W_n\rangle^{\text{gluon-loop}} = 8c_8\oint dz_i^\mu dz_j^\nu\int d^dx d^dy \epsilon^{\alpha\beta\gamma}\epsilon^{\delta\sigma\tau}\langle A_\mu A_\alpha\rangle\langle A_\nu A_\delta\rangle\langle A_\beta A_\tau\rangle\langle A_\gamma A_\sigma\rangle\,. \qquad \text{(B.31)}$$

To proceed, we recall the relation (A.16) between gauge field and ghost propagator and write

$$\begin{aligned}\epsilon^{\alpha\beta\gamma}\epsilon^{\delta\sigma\tau}\langle A_\beta A_\tau\rangle\langle A_\gamma A_\sigma\rangle &= \frac{1}{4}\,\epsilon^{\alpha\beta\gamma}\epsilon^{\delta\sigma\tau}\epsilon_{\beta\tau\kappa}\epsilon_{\gamma\sigma\rho}\partial_x^\rho\langle c(x)\bar c(y)\rangle\partial_x^\kappa\langle c(x)\bar c(y)\rangle\\ &= \frac{1}{2}\partial_x^\rho\langle c(x)\bar c(y)\rangle\partial_y^\kappa\langle c(x)\bar c(y)\rangle \qquad \text{(B.32)}\end{aligned}$$

where we used $\epsilon^{\alpha\beta\gamma}\epsilon^{\delta\sigma\tau}\epsilon_{\beta\tau\kappa}\epsilon_{\gamma\sigma\rho} = -\left(\eta^\alpha_\kappa\eta^\delta_\rho + \eta^\alpha_\rho\eta^\delta_\kappa\right)$ and $\partial_x F(x-y) = -\partial_y F(x-y)$ in the last step.

B.2.2 Ghost loop

The ghost loop diagram arises from contraction of the second order perturbation theory expansion of the gauge-field-ghost vertex term

$$\begin{aligned}\langle W_n\rangle^{\text{ghost loop}} &= \frac{1}{N}\langle \mathrm{Tr}\,(-\oint dz_i^\mu dz_j^\nu A_\mu A_\nu)\left(-\frac{1}{2!}\right)\left(\frac{k}{4\pi}\int d^dx\,\mathrm{Tr}\,(\partial^\mu\bar c\, i[A_\mu, c])\right)^2\rangle \qquad \text{(B.33)}\\ &= 2c_8\oint dz_i^\mu dz_j^\nu\int d^dx d^dy\langle \mathrm{Tr}\,(A_\mu A_\nu)\mathrm{Tr}\,(\partial_x^\rho\bar c A_\rho c)\mathrm{Tr}\,(\partial_y^\sigma\bar c A_\sigma c)\rangle\end{aligned}$$

where c_8 ist the same as defined above and the factor of 2 is due to the fact that the evaluation of the first line yields two identical planar diagrams that are kept and two identical non-planar diagrams that we drop. Contracting A_μ either with the x- or y-dependent vertex, we get a symmetry factor of 2. There is only one way for the remaining contractions and thus we get

$$\langle W_n\rangle^{\text{ghost loop}} = -4c_8 \oint dz_i^\mu dz_j^\nu \int d^dx d^dy \langle A_\mu A_\sigma\rangle\langle A_\nu A_\rho\rangle \partial_x^\rho \langle c(y)\bar{c}(x)\rangle \partial_y^\sigma \langle c(x)\bar{c}(y)\rangle \tag{B.34}$$

where a factor of -1 due to the anti-commuting ghost fields in the loop was taken into account. Summing up (B.31) and (B.34) we get

$$\langle W_n\rangle^{\text{gauge field loop}} + \langle W_n\rangle^{\text{ghost loop}} = 0\,. \tag{B.35}$$

The same relation (A.16) can be used to show the vanishing for the dilatation and special conformal Ward identities.

B.3 Conformal Ward identity

B.3.1 Insertion of the interaction term

We can rewrite (4.13) as

$$I'_{321} = \frac{1}{(d-2)^2}\int d^3s_{1,2,3}\epsilon(p_1,p_2,\partial_{z_1})\epsilon(p_3,p_2,\partial_{z_2})\int d^dx \frac{(x+z_2)^\nu}{|x|^d|x-z_{12}|^{d-2}|x-z_{32}|^{d-2}}\,. \tag{B.36}$$

Introducing Feynman parameters, changing the integration variable to $l = x-\beta_1 z_{12}-\beta_3 z_{32}$, using the same notation as in app. B.1, integrating over l and evaluating the action of the derivatives yields

$$\begin{aligned} I'_{321} = \frac{c_1}{(d-2)^2}\int d^3s_{1,2,3}\int d[\beta]_3\Big((\beta_1 z_1+\beta_2 z_2+\beta_3 z_3)^\nu \epsilon(p_1,p_2,\partial_{z_1})\epsilon(p_3,p_2,\partial_{z_2})\frac{1}{\Delta^{d-2}} \\ + \epsilon(p_1,p_2,p_3)2\beta_1\beta_3\epsilon_{\alpha\beta}{}^\nu p_2^\beta\,(\beta_1 p_1^\alpha \bar{s}_1+\beta_3 p_3^\alpha s_3)\,\frac{(2-d)}{\Delta^{d-1}}\Big)\,, \end{aligned} \tag{B.37}$$

The last term can be shown to be finite and the first term is very similar to the vertex diagram. Evaluation of the derivatives as in B.1 yields

$$\begin{aligned} I'_{321} = c_2 st\int_0^1 d^3s_{1,2,3}d^3\beta_{1,2,3}(\beta_1\beta_2\beta_3)^{(d-2)/2}\delta(\sum_i\beta_i-1) \\ (\beta_1 z_1+\beta_2 z_2+\beta_3 z_3)^\nu\left(\frac{1}{\Delta^{d-1}}-2\frac{(d-1)}{\Delta^d}\beta_1\beta_3\bar{s}_1 s_3(s+t)\right)+\text{finite}\,. \end{aligned} \tag{B.38}$$

It can be shown, e.g. using the Mellin Barnes technique as in B.1, that all divergent contributions are due to the first term. We have the following divergent contributions:

$$\begin{aligned} st\int d^3sd[\beta]_3\beta_1\beta_2\beta_3\left(\frac{\beta_1 z_1}{\Delta^{d-1}}\right) &= \frac{1}{\epsilon}\,a\,x_2^\nu + \mathcal{O}(\epsilon^0)\,, \\ st\int d^3sd[\beta]_3\beta_1\beta_2\beta_3\left(\frac{\beta_2 z_2}{\Delta^{d-1}}\right) &= \frac{1}{\epsilon}\,b\,(x_2^\nu + x_3^\nu) + \mathcal{O}(\epsilon^0)\,, \\ st\int d^3sd[\beta]_3\beta_1\beta_2\beta_3\left(\frac{\beta_3 z_3}{\Delta^{d-1}}\right) &= \frac{1}{\epsilon}\,(a\,x_3^\nu) + \mathcal{O}(\epsilon^0)\,. \end{aligned} \tag{B.39}$$

Numerical evaluation yields

$$a = 1.8562 \pm 0.0001\,, \quad b = 2.4989 \pm 0.0001\,. \tag{B.40}$$

To good accuracy we find

$$a + b = 4.35517 \pm 0.0002 \approx 2\pi\ln(2) = 4.35517...\,. \tag{B.41}$$

Summarising I'_{321} then reads

$$I'_{321} = \frac{c_2}{\epsilon}(a+b)(x_2+x_3)^\nu + \mathcal{O}(\epsilon^0) \approx \frac{2\pi i\ln(2)}{\epsilon}(x_2+x_3)^\nu + \mathcal{O}(\epsilon^0)\,. \tag{B.42}$$

B.3.2 Insertion of the kinetic term into the vertex diagram

For the kinetic insertion into the vertex diagram we have (4.16)

$$\begin{aligned} \langle\mathcal{L}(x)W_4\rangle^{(2)}_{(c)} = &\underbrace{\left(\frac{N}{k}\right)^2\frac{i}{8\pi^2}\left(\frac{\Gamma\left(\frac{d}{2}\right)}{\pi^{\frac{d-2}{2}}}\right)^4}_{=:c_3}\int d^dw\oint dz^{\mu\nu\rho}_{i,j,k}\epsilon^{\delta\sigma\tau}I_{\nu\sigma}\,G_{\mu\tau}(z_i-w)G_{\rho\delta}(z_k-w) \\ &+ \text{cyclic}(\mu,\nu,\rho;z_i,z_j,z_k) \end{aligned} \tag{B.43}$$

where $G_{\mu\nu}(x-y) = \epsilon_{\mu\nu\rho}\frac{(x-y)^\rho}{(-(x-y)^2)^{\frac{d}{2}}}$ and

$$I_{\nu\sigma}(x-z_j,x-w) = \epsilon^{\alpha\beta\gamma}\left(G_{\alpha\nu}(x-z_j)\partial^{(x)}_\beta G_{\gamma\sigma}(x-w) + G_{\alpha\sigma}(x-w)\partial^{(x)}_\beta G_{\gamma\nu}(x-z_j)\rangle\right)\,. \tag{B.44}$$

and the two other contractions are contained in cyclic$(\mu,\nu,\rho;z_i,z_j,z_k)$. For the dilatation Ward identity the integration over x can be performed by introducing two Feynman parameters. The result simply yields a propagator

$$\int d^dx\,I_{\nu\sigma} = -\frac{4\pi^{\frac{d}{2}}}{\Gamma\left(\frac{d}{2}\right)}\epsilon_{\nu\sigma\varphi}\frac{(z_j-w)^\varphi}{(-(z_j-w)^2)^{\frac{d}{2}}} = -\frac{4\pi^{\frac{d}{2}}}{\Gamma\left(\frac{d}{2}\right)}G_{\nu\sigma}(z_j-w)\,, \tag{B.45}$$

In the case of the special conformal Ward identity the integration is a little more involved. The integral over d^dx can be solved by introducing Feynman parameters and after some algebra one finds

$$\begin{aligned}\int d^dx\, x^\lambda \langle \mathcal{L}(x) W_4\rangle^{(2)}_{(c)} = 2c_3c_4 \oint dz^{\mu,\nu,\rho}_{i,j,k} \int d^dw \epsilon^{\delta\sigma\tau}\epsilon^{\alpha\beta\gamma}\epsilon_{\alpha\nu\xi}\epsilon_{\gamma\sigma\varphi} \\ \partial^\xi\left((2\eta^{\varphi\lambda}\partial_\beta + \eta^\lambda_\beta\partial^\varphi)\left(\frac{1}{((z_j-w)^2)^{\frac{d}{2}-2}}\right) - \partial^\varphi\partial_\beta\left(\frac{(z_j+w)^\lambda}{((z_j-w)^2)^{\frac{d}{2}-2}}\right)\right) \\ G_{\rho\delta}G_{\mu\tau} + \text{cyclic}(\mu,\nu,\rho;z_i,z_j,z_k)\,,\end{aligned} \tag{B.46}$$

where all derivatives are taken with respect to z_j and c_4 is a constant obtained through integration over d^dx. Inserting the propagators we can write this in a form convenient to solve the integral over d^dw

$$2c_3c_4 \oint dz^{\mu,\nu,\rho}_{i,j,k}\epsilon^{\delta\sigma\tau}\epsilon^{\alpha\beta\gamma}\epsilon_{\alpha\nu\xi}\epsilon_{\gamma\sigma\varphi}\epsilon_{\rho\delta\chi}\epsilon_{\mu\tau\theta}\partial^\theta_i\partial^\xi_j\partial^\chi_k\left((2\eta^{\varphi\lambda}\partial_{j,\beta}+\eta^\lambda_\beta\partial^\varphi_j)J_j - \partial^\varphi_j\partial_{\beta,j}J^\lambda_j\right) + \text{cyclic} \tag{B.47}$$

where the integrals read

$$\begin{aligned}J_j &= \frac{1}{(2-d)^2}\int d^dw \frac{1}{((z_j-w)^2)^{\frac{d}{2}-2}((z_i-w)^2)^{\frac{d}{2}-1}((z_k-w)^2)^{\frac{d}{2}-1}} \\ J^\lambda_j &= \frac{1}{(2-d)^2}\int d^dw \frac{(z_j+w)^\lambda}{((z_j-w)^2)^{\frac{d}{2}-2}((z_i-w)^2)^{\frac{d}{2}-1}((z_k-w)^2)^{\frac{d}{2}-1}}\end{aligned} \tag{B.48}$$

The integrations over w can be performed by introducing three Feynman parameters β_i and we get

$$J_j = c_5\int d[\beta]_{3,j}\left(\frac{1}{\Delta}\right)^{d-4}, \qquad J^\lambda_j = c_5\int d[\beta]_{3,j}(z_j+\sum_i\beta_i z_i)^\lambda\left(\frac{1}{\Delta}\right)^{d-4} \tag{B.49}$$

where

$$\int d[\beta]_{3,j} = \int_0^1 d\beta_i d\beta_j d\beta_k \delta\left(\sum_i\beta_i - 1\right)(\beta_i\beta_j\beta_k)^{\frac{d}{2}-2}\,\beta_j^{-1} \tag{B.50}$$

and c_5 is a constant obtained by integrating over w, the product $c_3c_4c_5$ is explicitly given below. The expression for Δ is the same as in (B.4) For the cyclic permutations we can use the same expression, replacing the measure with $d[\beta]_{3,i}$ respectively $d[\beta]_{3,k}$, i.e. exchanging β_j^{-1} with β_i^{-1} respectively β_k^{-1} in (B.50).

All three contributions can then be written as

$$\begin{aligned}2c_3c_4c_5 \oint dz^{\mu,\nu,\rho}_{i,j,k}\epsilon^{\delta\sigma\tau}\epsilon^{\alpha\beta\gamma}\epsilon_{\gamma\sigma\varphi}\Big(&\epsilon_{\alpha\mu\xi}\epsilon_{\nu\delta\chi}\epsilon_{\rho\tau\theta}\partial^\theta_k\partial^\xi_i\partial^\chi_j\left((2\eta^{\varphi\lambda}\partial_{i,\beta}+\eta^\lambda_\beta\partial^\varphi_i)J_i - \partial^\varphi_i\partial_{\beta,i}J^\lambda_i\right) \\ &\epsilon_{\alpha\nu\xi}\epsilon_{\rho\delta\chi}\epsilon_{\mu\tau\theta}\partial^\theta_i\partial^\xi_j\partial^\chi_k\left((2\eta^{\varphi\lambda}\partial_{j,\beta}+\eta^\lambda_\beta\partial^\varphi_j)J_j - \partial^\varphi_j\partial_{\beta,j}J^\lambda_j\right) \\ &\epsilon_{\alpha\rho\xi}\epsilon_{\mu\delta\chi}\epsilon_{\nu\tau\theta}\partial^\theta_j\partial^\xi_k\partial^\chi_i\left((2\eta^{\varphi\lambda}\partial_{k,\beta}+\eta^\lambda_\beta\partial^\varphi_k)J_k - \partial^\varphi_k\partial_{\beta,k}J^\lambda_k\right)\Big)\end{aligned} \tag{B.51}$$

and where

$$2c_3c_4c_5 = i\frac{\pi^{2-d}}{128}\left(\frac{N}{k}\right)^2 \Gamma(d-4) \tag{B.52}$$

We can evaluate the derivatives and contractions with the computer and find that the non-vanishing contributions have the structure

$$\int d^dx\, x^\lambda \langle \mathcal{L}(x) W_4\rangle^{\text{vertex-insertion}} = \left(\frac{N}{k}\right)^2 \sum_{i>j>k} \int_0^1 ds_{i,j,k} \int d[\beta]_3 \left(I^\lambda_{ijk,-d-1} + I^\lambda_{ijk,-d} + I^\lambda_{ijk,-d+1}\right) \tag{B.53}$$

where $I_{ijk,p}$ are lengthy terms proportional to $1/\Delta^p$.

For the conformal Ward identity we are only interested in the divergent part of the above quantities, which can be automatically extracted with the Mellin-Barnes technique. We find that all terms vanish except for $i \neq j \neq k$. Specialising to the case $i = 3, j = 2, k = 1$ we find

$$\begin{aligned} \int I^\lambda_{312,-d-1} &= \mathcal{O}(\epsilon^0)\,, \\ \int I^\lambda_{312,-d} &= \frac{i}{\epsilon}(a_1 x_2^\lambda + a_2 x_3^\lambda) + \mathcal{O}(\epsilon^0)\,, \\ \int I^\lambda_{321,-d+1} &= \frac{i}{\epsilon}(b_1 x_2^\lambda + b_2 x_3^\lambda) + \mathcal{O}(\epsilon^0)\,. \end{aligned} \tag{B.54}$$

Numerical evaluation of the integrals yields

$$\begin{aligned} a_1 &= 0.3465735 \pm 10^{-6} \approx \frac{1}{2}\ln(2) = 0.3465735...\,, \\ a_2 &= 0.3465735 \pm 8\cdot 10^{-7} \approx \frac{1}{2}\ln(2) = 0.3465735...\,, \\ b_1 &= -0.8664339 \pm 14\cdot 10^{-7} \approx -\frac{5}{4}\ln(2) = -0.86643397...\,, \\ b_2 &= -0.8664339 \pm 10^{-6} \approx -\frac{5}{4}\ln(2) = -0.86643397...\,. \end{aligned} \tag{B.55}$$

Adding up the results, summing over all four diagrams and taking into account the corresponding prefactors we get

$$\int d^dx\, x^\lambda \langle \mathcal{L}(x) W_4\rangle^{(2)}_{(c)} \approx -i\frac{3}{4}\frac{\ln(2)}{\epsilon}\left(\sum_i x_i^\lambda\right) + \mathcal{O}(\epsilon^0)\,. \tag{B.56}$$

C One loop gauge field propagator in ABJM theory

Here we review the calculation of the one-loop correction to the gauge field propagator, see also [6]. We have fermionic and bosonic contributions in the loop and thus

$$G^{(1)}_{\mu\nu}(p) = G^{(F,1)}_{\mu\nu}(p) + G^{(B,1)}_{\mu\nu}(p) \tag{C.1}$$

where

$$G^{(1)}_{\mu\nu}(p) = \left(\frac{2\pi}{k}\right)^2 \frac{\epsilon_{\mu\rho\kappa}p^\kappa}{p^2}\left(\Pi^{(B)}_{\rho\lambda}(p) + \Pi^{(F)}_{\rho\lambda}(p)\right)\frac{\epsilon_{\lambda\nu\delta}p^\delta}{p^2} \tag{C.2}$$

and

$$\begin{aligned}\Pi^{(B)}_{\mu\nu}(p) &= +N\delta^I_I\mu^{2\epsilon}\int\frac{d^dk}{(2\pi)^d}\frac{(2k+p)_\mu(2k+p)_\nu}{k^2(p+k)^2} \\ \Pi^{(F)}_{\mu\nu}(p) &= -N\delta^I_I\mu^{2\epsilon}\int\frac{d^dk}{(2\pi)^d}\frac{\mathrm{Tr}\ (\gamma_\mu(\not{p}+\not{k})\gamma_\nu\not{k})}{k^2(p+k)^2}\,.\end{aligned} \tag{C.3}$$

We use the DRED scheme for Dirac matrix operations as well as for Levi-Civita tensor contractions, i.e. we work in strictly $d = 3$ to obtain scalar integrands and only then continue the loop momenta to d-dimensional space to perform the integrals in d dimensions. This scheme has been shown to respect the Slavnov-Taylor identities up to two loop order in [35].

Then we have

$$\mathrm{Tr}\ (\gamma_\mu(\not{p}+\not{k})\gamma_\nu\not{k}) = 2\left(-\eta_{\mu\nu}(p+k)\cdot k + 2k_\mu k_\nu + p_\mu k_\nu + p_\mu k_\nu\right)\,. \tag{C.4}$$

The last two terms can be dropped, since they vanish when contracted with (C.2). The same is true for terms proportional to p_μ, p_ν in the bosonic term.

Summing up all remaining terms we get

$$+\,N\delta^I_I\mu^{2\epsilon}2\eta_{\mu\nu}\int\frac{d^dk}{(2\pi)^d}\frac{k\cdot(p+k)}{k^2(p+k)^2} \tag{C.5}$$

Introducing Feynman parameters, we have

$$+N\delta^I_I\mu^{2\epsilon}2\eta_{\mu\nu}\int_0^1 d\alpha\int\frac{d^dk}{(2\pi)^d}\frac{k\cdot(p+k)}{[(k+\bar\alpha p)^2-\Delta]^2} \tag{C.6}$$

where $\Delta = -\alpha\bar\alpha p^2$. Then, we shift $k = l - \bar\alpha p$ and drop terms linear in l_μ

$$+N\delta^I_I\mu^{2\epsilon}2\eta_{\mu\nu}\int_0^1 d\alpha\int\frac{d^dl}{(2\pi)^d}\frac{l^2-\alpha\bar\alpha p^2}{[l^2-\Delta]^2}\,. \tag{C.7}$$

Using the standard integrals

$$\int\frac{d^dl}{(2\pi)^d}\frac{l^2}{[l^2-\Delta]^2} = -\frac{i}{(4\pi)^{\frac{d}{2}}}\frac{d}{2}\frac{\Gamma(1-\frac{d}{2})}{(\Delta)^{1-\frac{d}{2}}} \qquad \int\frac{d^dl}{(2\pi)^d}\frac{1}{[l^2-\Delta]^2} = \frac{i}{(4\pi)^{\frac{d}{2}}}\frac{\Gamma(2-\frac{d}{2})}{(\Delta)^{2-\frac{d}{2}}} \tag{C.8}$$

and $\epsilon_{\lambda\kappa\mu}\epsilon_{\lambda\nu\delta} = \eta_{\kappa\nu}\eta_{\mu\delta} - \eta_{\kappa\delta}\eta_{\mu\nu}$ we get

$$G^{(1)}_{\mu\nu}(p) = \left(N\delta^I_I\mu^{2\epsilon}2\frac{(-i)}{(4\pi)^{\frac{d}{2}}}\frac{\Gamma(1-\frac{d}{2})\Gamma(\frac{d}{2})^2}{\Gamma(d-1)}\right)\left(\frac{2\pi}{k}\right)^2\frac{1}{(-p^2)^{3-\frac{d}{2}}}\left(p_\mu p_\nu - \eta_{\mu\nu}p^2\right)\,. \tag{C.9}$$

The standard formula[10]

$$\int \frac{d^d p}{(2\pi)^d} \frac{e^{-ipx}}{(-p^2)^k} = i \frac{\Gamma(\frac{d}{2}-k)}{\Gamma(k)} \frac{1}{4^k \pi^{\frac{d}{2}}} \frac{1}{(-x^2)^{\frac{d}{2}-k}} \tag{C.10}$$

leads to the Fourier transform of (C.9)

$$\begin{aligned} G^{(1)}_{\mu\nu}(x) &= \mu^{2\epsilon} \int \frac{d^d p}{(2\pi)^d} G^{(1)}_{\mu\nu}(p) e^{-ipx} \qquad (C.11) \\ &= \left(\frac{2\pi}{k}\right)^2 \frac{N\delta^I_I}{8} \frac{\Gamma(1-\frac{d}{2})\Gamma(\frac{d}{2})^2}{\Gamma(d-1)} \frac{(\mu^{2\epsilon})^2}{\pi^d} \left(\frac{\Gamma(d-2)}{\Gamma(2-\frac{d}{2})} \frac{\eta_{\mu\nu}}{(-x^2)^{d-2}} - \partial_\mu \partial_\nu \left(\frac{\Gamma(d-3)}{\Gamma(3-\frac{d}{2})} \frac{1}{4} \frac{1}{(-x^2)^{d-3}} \right) \right) \end{aligned}$$

References

[1] E. Witten, *"Quantum field theory and the Jones polynomial"*, Commun. Math. Phys. 121, 351 (1989).

[2] E. Guadagnini, M. Martellini and M. Mintchev, *"Wilson Lines in Chern-Simons Theory and Link Invariants"*, Nucl. Phys. B330, 575 (1990).

[3] M. Alvarez and J. M. F. Labastida, *"Analysis of observables in Chern-Simons perturbation theory"*, Nucl. Phys. B395, 198 (1993), `hep-th/9110069`.

[4] J. M. F. Labastida, *"Chern-Simons gauge theory: Ten years after"*, `hep-th/9905057`.

[5] O. Aharony, O. Bergman, D. L. Jafferis and J. Maldacena, *"$\mathcal{N} = 6$ superconformal Chern-Simons-matter theories, M2-branes and their gravity duals"*, JHEP 0810, 091 (2008), `arxiv:0806.1218`.

[6] N. Drukker, J. Plefka and D. Young, *"Wilson loops in 3-dimensional N=6 supersymmetric Chern- Simons Theory and their string theory duals"*, JHEP 0811, 019 (2008), `arxiv:0809.2787`.

[7] B. Chen and J.-B. Wu, *"Supersymmetric Wilson Loops in N=6 Super Chern-Simons- matter theory"*, Nucl. Phys. B825, 38 (2010), `arxiv:0809.2863`.

[8] S.-J. Rey, T. Suyama and S. Yamaguchi, *"Wilson Loops in Superconformal Chern-Simons Theory and Fundamental Strings in Anti-de Sitter Supergravity Dual"*, JHEP 0903, 127 (2009), `arxiv:0809.3786`.

[9] N. Drukker and D. Trancanelli, *"A supermatrix model for N=6 super Chern-Simons-matter theory"*, JHEP 1002, 058 (2010), `arxiv:0912.3006`.

[10] M. Marino and P. Putrov, *"Exact Results in ABJM Theory from Topological Strings"*, `arxiv:0912.3074`.

[11] A. Kapustin, B. Willett and I. Yaakov, *"Exact Results for Wilson Loops in Superconformal Chern- Simons Theories with Matter"*, JHEP 1003, 089 (2010), `arxiv:0909.4559`.

[12] L. F. Alday and J. M. Maldacena, *"Gluon scattering amplitudes at strong coupling"*, JHEP 0706, 064 (2007), `arxiv:0705.0303`.

[10] For $\eta_{\mu\nu} = diag\,(1,-1,-1)$

[13] J. M. Drummond, G. P. Korchemsky and E. Sokatchev, *"Conformal properties of four-gluon planar amplitudes and Wilson loops"*, Nucl. Phys. B795, 385 (2008), arxiv:0707.0243.

[14] A. Brandhuber, P. Heslop and G. Travaglini, *"MHV Amplitudes in $\mathcal{N} = 4$ Super Yang–Mills and Wilson Loops"*, Nucl. Phys. B794, 231 (2008), arxiv:0707.1153.

[15] J. M. Drummond, J. Henn, G. P. Korchemsky and E. Sokatchev, *"On planar gluon amplitudes/Wilson loops duality"*, Nucl. Phys. B795, 52 (2008), arxiv:0709.2368.

[16] J. M. Drummond, J. Henn, G. P. Korchemsky and E. Sokatchev, *"Dual superconformal symmetry of scattering amplitudes in $\mathcal{N} = 4$ super-Yang–Mills theory"*, Nucl. Phys. B828, 317 (2010), arxiv:0807.1095.

[17] J. M. Drummond, J. M. Henn and J. Plefka, *"Yangian symmetry of scattering amplitudes in $\mathcal{N} = 4$ super Yang-Mills theory"*, JHEP 0905, 046 (2009), arxiv:0902.2987.

[18] L. F. Alday and R. Roiban, *"Scattering Amplitudes, Wilson Loops and the String/Gauge Theory Correspondence"*, Phys. Rept. 468, 153 (2008), arxiv:0807.1889.

[19] J. M. Henn, *"Duality between Wilson loops and gluon amplitudes"*, Fortschr. Phys. 57, 729 (2009), arxiv:0903.0522.

[20] J. A. Minahan and K. Zarembo, *"The Bethe-ansatz for $\mathcal{N} = 4$ super Yang-Mills"*, JHEP 0303, 013 (2003), hep-th/0212208.

[21] N. Beisert and M. Staudacher, *"The $\mathcal{N} = 4$ SYM Integrable Super Spin Chain"*, Nucl. Phys. B670, 439 (2003), hep-th/0307042.

[22] N. Beisert, C. Kristjansen and M. Staudacher, *"The Dilatation Operator of $\mathcal{N} = 4$ Conformal Super Yang-Mills Theory"*, Nucl. Phys. B664, 131 (2003), hep-th/0303060.

[23] I. Bena, J. Polchinski and R. Roiban, *"Hidden symmetries of the $AdS_5 \times S^5$ superstring"*, Phys. Rev. D69, 046002 (2004), hep-th/0305116.

[24] A. A. Tseytlin, *"Semiclassical strings in $AdS_5 \times S^5$ and scalar operators in $\mathcal{N} = 4$ SYM theory"*, Comptes Rendus Physique 5, 1049 (2004), hep-th/0407218.

[25] A. V. Belitsky, V. M. Braun, A. S. Gorsky and G. P. Korchemsky, *"Integrability in QCD and beyond"*, Int. J. Mod. Phys. A19, 4715 (2004), hep-th/0407232.

[26] N. Beisert, *"The Dilatation Operator of $\mathcal{N} = 4$ Super Yang-Mills Theory and Integrability"*, Phys. Rept. 405, 1 (2004), hep-th/0407277.

[27] N. Beisert, *"Higher-Loop Integrability in $\mathcal{N} = 4$ Gauge Theory"*, Comptes Rendus Physique 5, 1039 (2004), hep-th/0409147.

[28] K. Zarembo, *"Semiclassical Bethe ansatz and AdS/CFT"*, Comptes Rendus Physique 5, 1081 (2004), hep-th/0411191.

[29] J. Plefka, *"Spinning strings and integrable spin chains in the AdS/CFT correspondence"*, Living. Rev. Relativity 8, 9 (2005), hep-th/0507136.

[30] J. A. Minahan, *"A brief introduction to the Bethe ansatz in $\mathcal{N} = 4$ super-Yang-Mills"*, J. Phys. A39, 12657 (2006).

[31] G. Arutyunov and S. Frolov, *"Foundations of the $AdS_5 \times S^5$ Superstring. Part I"*, J. Phys. A42, 254003 (2009), arxiv:0901.4937.

[32] J. A. Minahan and K. Zarembo, *"The Bethe ansatz for superconformal Chern-Simons"*, JHEP 0809, 040 (2008), arxiv:0806.3951.

[33] N. Gromov and P. Vieira, *"The all loop AdS4/CFT3 Bethe ansatz"*, JHEP 0901, 016 (2009), arxiv:0807.0777.

[34] A. Agarwal, N. Beisert and T. McLoughlin, *"Scattering in Mass-Deformed N¿=4 Chern-Simons Models"*, JHEP 0906, 045 (2009), arxiv:0812.3367.

[35] W. Chen, G. W. Semenoff and Y.-S. Wu, *"Two loop analysis of non Abelian Chern-Simons theory"*, Phys. Rev. D46, 5521 (1992), hep-th/9209005.

[36] N. Berkovits and J. Maldacena, *"Fermionic T-Duality, Dual Superconformal Symmetry, and the Amplitude/Wilson Loop Connection"*, JHEP 0809, 062 (2008), arxiv:0807.3196.

[37] N. Beisert, R. Ricci, A. A. Tseytlin and M. Wolf, *"Dual Superconformal Symmetry from $AdS_5 \times S^5$ Superstring Integrability"*, Phys. Rev. D78, 126004 (2008), arxiv:0807.3228.

[38] I. Adam, A. Dekel and Y. Oz, *"On Integrable Backgrounds Self-dual under Fermionic T-duality"*, JHEP 0904, 120 (2009), arxiv:0902.3805.

[39] G. Arutyunov and S. Frolov, *"Superstrings on $AdS_4 \times CP^3$ as a Coset Sigma-model"*, JHEP 0809, 129 (2008), arxiv:0806.4940.

[40] B. Stefanski, jr, *"Green-Schwarz action for Type IIA strings on $AdS_4 \times CP^3$"*, Nucl. Phys. B808, 80 (2009), arxiv:0806.4948.

[41] P. A. Grassi, D. Sorokin and L. Wulff, *"Simplifying superstring and D-brane actions in $AdS_4 x CP^3$ superbackground"*, JHEP 0908, 060 (2009), arxiv:0903.5407.

[42] J. Gomis, D. Sorokin and L. Wulff, *"The Complete AdS(4) x CP**3 superspace for the type IIA superstring and D-branes"*, JHEP 0903, 015 (2009), arxiv:0811.1566.

[43] T. Bargheer, F. Loebbert and C. Meneghelli, *"Symmetries of Tree-level Scattering Amplitudes in N=6 Superconformal Chern-Simons Theory"*, arxiv:1003.6120.

[44] W.-M. Chen and Y.-t. Huang, *"Dualities for Loop Amplitudes of N=6 Chern-Simons Matter Theory"*, arxiv:1107.2710, * Temporary entry *.

[45] M. S. Bianchi, M. Leoni, A. Mauri, S. Penati and A. Santambrogio, *"Scattering Amplitudes/Wilson Loop Duality In ABJM Theory"*, arxiv:1107.3139.

[46] J. M. Drummond, J. Henn, G. P. Korchemsky and E. Sokatchev, *"Conformal Ward identities for Wilson loops and a test of the duality with gluon amplitudes"*, Nucl. Phys. B826, 337 (2010), arxiv:0712.1223.

[47] S. Sarkar, *"Dimensional Regularization and Broken Conformal Ward Identities"*, Nucl. Phys. B83, 108 (1974).

[48] V. M. Braun, G. P. Korchemsky and D. Muller, *"The uses of conformal symmetry in QCD"*, Prog. Part. Nucl. Phys. 51, 311 (2003), hep-ph/0306057.

[49] D. Gaiotto and X. Yin, *"Notes on superconformal Chern-Simons-Matter theories"*, JHEP 0708, 056 (2007), arxiv:0704.3740.

[50] D. Bak and S.-J. Rey, *"Integrable Spin Chain in Superconformal Chern-Simons Theory"*, JHEP 0810, 053 (2008), arxiv:0807.2063.

[51] V. Smirnov, *"Feynman integral calculus"*, Springer Verlag (2006).

[52] M. Czakon, *"Automatized analytic continuation of Mellin-Barnes integrals"*, Comput. Phys. Commun. 175, 559 (2006), `hep-ph/0511200`.